

# Author's response on the revised manuscript "Impact of reactive surfaces on the abiotic reaction between nitrite and ferrous iron and associated nitrogen and oxygen isotope dynamics" by Anna-Neva Visser et al.

## 1. Point-by-Point response to the reviews

### 1.1. Response to comments by Anonymous Referee #1

First, we wish to thank the reviewer for his/her valuable inputs and comments on our manuscript.

L39-40: I'm surprised there are no older references to the role of iron.

Reply: We agree that indeed there are many more references regarding the role of iron in the environment. However, our choice can be considered as "best of" selection, covering a whole suite of different aspects: we choose (1) Expert et al., 2012 since they explicitly focus on the vital role of iron for all living organisms, its wide range of redox potentials and its catalytic role in various metabolic pathways; (2) Lovley et al., 1997, who reported on the importance of iron already in 1988, however, the publication chosen represents a nice "summary", focusing also on various reactions and thus its "remediative" capabilities. Obviously, we wanted to limit the number of references, but if the reviewer thinks of a specific publication, we will be happy to include it. Again, in light of the many publications on the importance of iron available, and since our manuscript is already very long, we simply decided to pick two references that support the statement/sentence.

General experiment setup section: The conditions of the experiment are anoxia and the addition of iron and nitrogen in the form of nitrite. Under these conditions, in the environment, it is conceivable that dissimilative reduction of nitrite to ammonium may occur. Of course under perfect abiotic conditions DNRA should not occur. Did the authors measure ammonium concentrations throughout the experiment to ensure that no other processes than the one under study were taking place?

Reply: As the reviewer stated, DNRA should not occur under abiotic conditions. Considering that the abiotic experiments were all performed under laboratory conditions, using a medium that contains already high amounts of ammonium (5.61 mM  $\text{NH}_4\text{Cl}$ , see 2.1), ammonium concentrations were only checked sporadically for some setups. Since only (if at all) minor fluctuations were observed, no further efforts to determine ammonium concentrations were attempted.

L120-121: How long does it take from incubation to the measurement of concentrations and isotopes? Light is a factor that can generate abiotic reactions, which in turn can generate isotope fractionation. What about it?

Reply: Yes, light-induced reactions have to be considered. That was one reason why nitrite concentrations were measured via CFA immediately after the samples were taken (within one hour). After determining the nitrite concentrations, the azide method was applied (within max. 2-3 hrs). Samples were kept inside the glovebox in coloured (dark brown or blue) Eppendorf tubes, whereas the latter were chosen to inhibit potential photocatalytic reactions. The azide-treated headspace vials were stored in card boxes at RT until measured. At this point, the sample is fixed (i.e., turned into  $\text{N}_2\text{O}$ ). Therefore, we are rather confident that neither light nor (possibly) temperature could have influenced the values. However, one could argue that the blue coloured Eppendorf tubes might not suffice, since they are indeed partly translucent. Since during one of the experiments blue and brown vials were used, and still, the concentration values within the nine replicates were very similar (see Figure 1 A and C,

note error bars), we are confident that the rapid processing and precautions taken to avoid light-induced reactions did indeed suffice.

L179-180: Two nitrite isotope standards have been used. What are the values of these standards? Do these values include those of the samples measured in this study? What is the analytical precision of the method (preparation + intrinsic analysis) for the determination of the isotopic composition of nitrite (15N and 18O)?

Reply: Standard N-7373 has a  $\delta^{15}\text{N}$  value of -79.6‰ and a  $\delta^{18}\text{O}$  value of +4.5‰. In contrast, standard N-10219 has a  $\delta^{15}\text{N}$  value of +2.8‰ and a  $\delta^{18}\text{O}$  value of +88.5‰. Using both standards allowed for the reliable correction using standard bracketing: The standard  $\delta^{15}\text{N}$  range included the  $\delta^{15}\text{N}$  values obtained for our samples perfectly. The  $\delta^{18}\text{O}$  values measured fell only slightly below (-0.5 to 2.5‰) the range given by the standards, so that corrections are reliable. Based on replicate measurements of laboratory standards and samples, the analytical precision for  $\text{NO}_2^-$   $\delta^{15}\text{N}$  and  $\delta^{18}\text{O}$  analyses was  $\pm 0.4\%$  and  $\pm 0.6\%$  (1 SD), respectively.

L285-291: Rayleigh conditions allow the isotope fractionation factor to be easily determined by looking at the slope of the line on a representation  $\ln C/C_0$  as a function of  $\delta^{15}\text{N}$ , but not C (with C the concentration at time t and  $C_0$  the initial concentration). This paragraph is not clear to me. Moreover, doesn't the fact that there is first a decrease of  $\delta^{15}\text{N}$ , i.e. an inverse isotopic fractionation, with a decrease of the amount of heavy isotope in the residual substrate, and then an enrichment, mean that several processes could take place and that process 1 takes place at the beginning of the experiment with a higher rate than the second process which either starts at the beginning of the experiment or when process 1 is completed? Very concretely, the trend line is calculated on the points starting from the lowest  $\delta^{15}\text{N}$  values? I think it would be necessary to clarify this part.

Reply: We agree, the title of the x-axis of Figure 5 might be misleading. Of course, the values of the x-axis represent the  $\ln$  of the substrate fraction remaining (as mentioned in the caption below the figure). Hence, it is the  $\ln(f)$  whereas f is  $C/C_0$ . We will change the title of the x-axis to avoid future confusions. With regards to the second comment, i.e., that the data presented might simply reflect that two different processes are at work, we also agree. However, since it is hard to explain which processes might be at work and if this is indeed a clear inverse effect, we decided to calculate the isotope effect using the lowest  $\delta^{15}\text{N}$  values observed (i.e. for the experimental period where we show a clear decline in nitrite concentration with a net increase in  $\delta^{15}\text{N}$ ). We will clarify that there is putative evidence for multiple processes occurring in the incubations, and that this has implications for the Rayleigh approach.

L296-302: Is it not possible to envisage that the variations in  $\delta^{18}\text{O}$  are due solely to an exchange between the oxygen of the nitrite and the oxygen of the water? By the way, what is the isotopic composition of water? Is it constant during the experiment?

Reply: Unfortunately, the isotopic composition of the water was not measured, and we can only assume its  $\delta^{18}\text{O}$  (the water used in Tübingen has a  $\delta^{18}\text{O}$  of roughly 11‰). It is possible that the variations in  $\delta^{18}\text{O}$  are partially attributable to oxygen atom exchange dynamics with the matrix (see e.g. L504-516). However, considering that the observed drop in  $\delta^{18}\text{O}$  values in both experiments occurs more or less simultaneously with the drop in  $\delta^{15}\text{N}$  might be indicative of other dynamics (e.g. sorption, complexation?).

L309-313: The authors have done a significant analytical work. Why not show the variations in  $\text{N}_2\text{O}$  concentration as a function of nitrite concentrations? Before any interpretation with isotopes or isotopologists, it seems to me useful and necessary to work on the concentrations and in particular to make mass balances.

Reply: The proposed graph could be added to the supplementary material. However, particularly for the mineral only setups, this way of visualizing the data does not help much (see graph added). Also, for the main manuscript we had severe concerns with regards to its length. Therefore, we chose to present only

graphs that really help to understand the main messages of this project. With regards to the mass balance: The initial objectives of this project included mass balance considerations since it was supposed to lay the ground for a following study on nitrate-dependent Fe(II) oxidation in selected microbial strains. Unfortunately, we did not have the capacities to also analyse the  $N_2$  samples, so a proper mass balance is unfortunately not possible.

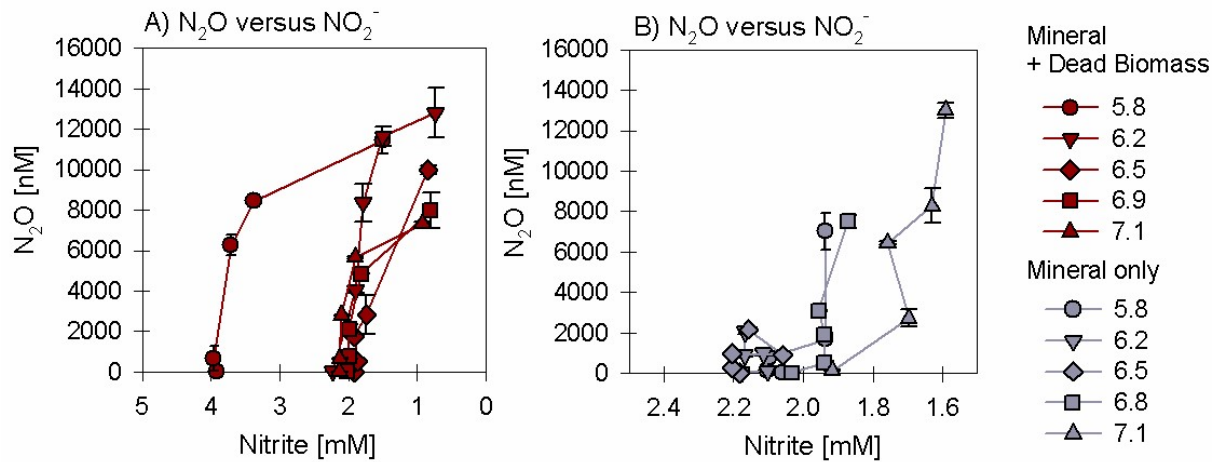


Figure 1:  $N_2O$  vs  $NO_2^-$  concentrations in (A) mineral plus dead biomass and (B) mineral only experiment

L314-315: The authors do not discuss the very negative SP value, which is very distinct from the other points. Is this an analytical problem?

Reply: We assume that the reviewer is referring to the observed drops in SP values (-120 to -80‰), occurring at  $t_1$  for samples taken from the mineral + dead biomass setup at pH 6.2 and mineral only at pH 5.8. After another thorough check of the raw data, we have to admit that for those particular samples the peak areas of the data obtained via CF-IRMS were much higher (compared to standards), possibly causing an extreme linearity or contamination effect that is affecting the data. We re-checked the entire data set again and removed these outliers (see revised figure below). The bulk of the data is not compromised, as we have good agreement between the standard and the sample peak areas.

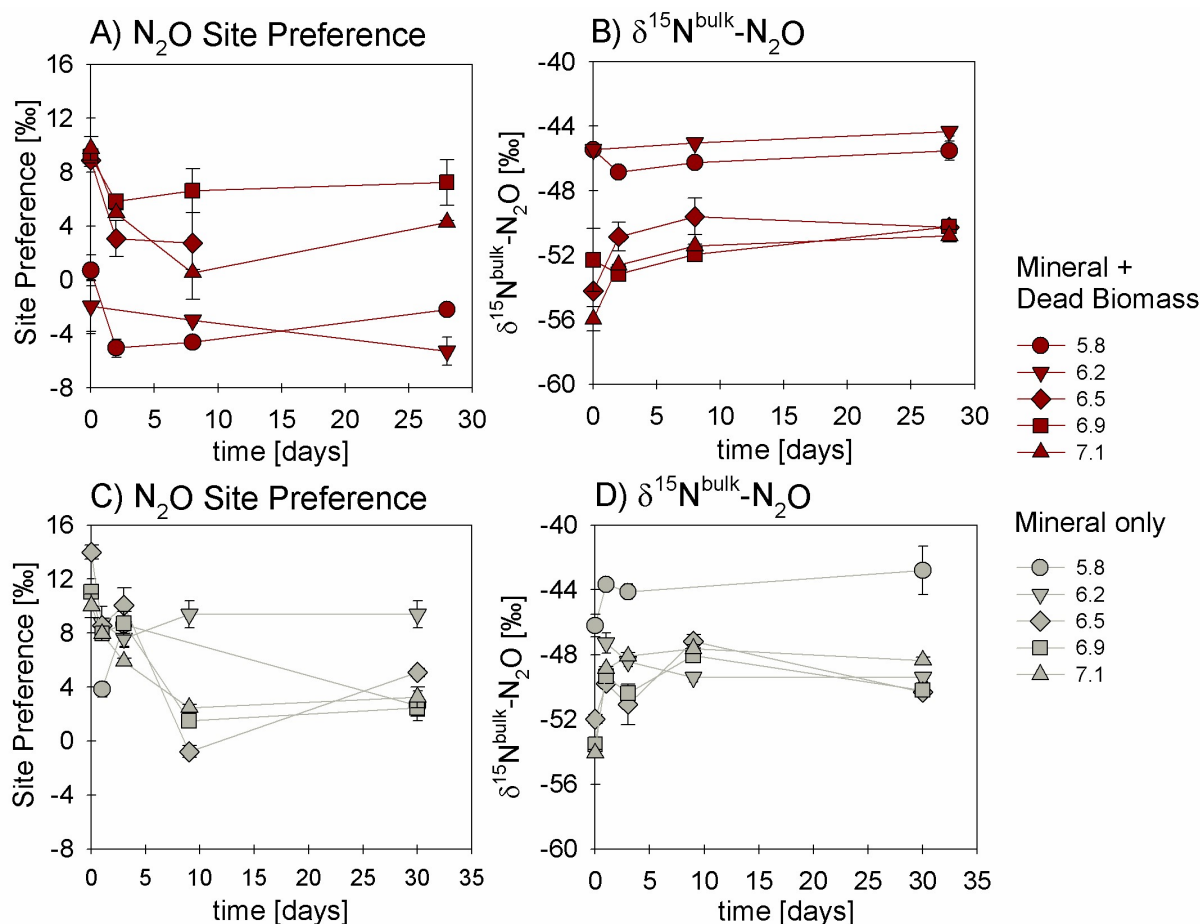


Figure 2: Site Preference (SP; A, C) and  $\delta^{15}\text{N}^{\text{bulk}}-\text{N}_2\text{O}$  (B, D) values of  $\text{N}_2\text{O}$  produced in experiments amended with mineral + dead biomass (red) and mineral-only (grey)

L326: There is no figure S6. But mentioned in S5 section figure 3.

Reply: We thank the reviewer for pointing this out and apologize for the mistake. Figure S5 mentioned in L322 actually corresponds to Figure S4 in the supplements, while S6 in L 326 refers to S5! We will change this in the re-submitted version of the MS.

L484-486: Large variations of  $\delta^{15}\text{N}$  are not associated with variations of  $\delta^{18}\text{O}$ . While these are measurements made on the residual substrate. The drop in  $\delta^{18}\text{O}$  at the beginning of the experiment is more likely due to an isotopic exchange with the oxygen in the water than evidence of a process.

Reply: Whether the drop is solely caused by the O isotopic exchange or, maybe partially, by interactions with the mineral surface, is not really clear. The drop observed in  $\delta^{18}\text{O}$  occurs almost simultaneously with the e.g. the decrease in  $\delta^{15}\text{N}$  for the mineral + dead biomass experiment. This might be indicative of other processes playing indeed a certain role. However, as we tried to explain in L496ff in the original MS, we assume that the main effect is the oxygen exchange with the water of the medium, which simply takes time and thus results in “fluctuations” (especially for the mineral only experiments) until the entire system is equilibrated.

L531-538: It might be interesting to look at  $\delta^{18}\text{O}$  variations of  $\text{N}_2\text{O}$  during the experiment. And see if it correlates with that of nitrite. This would also be an opportunity to confirm or deny whether there is an isotope exchange between the oxygen in the nitrite and the oxygen in the water.

Reply: Indeed, using the  $\delta^{18}\text{O}$  variations of  $\text{N}_2\text{O}$  might help to better understand the isotope exchange processes within the system. However, since  $\text{N}_2\text{O}$  is definitely not the only product and possibly further

reduced (resulting in a branching effect caused by the removed O atoms, which is further affecting the O dynamics within the system), this approach would be biased.

L551-552: if N<sub>2</sub>O is considered to accumulate, it can be considered to be the accumulated product in the case of a Rayleigh distillation. In this case, and taking into account the isotope fractionation associated with nitrite reduction, it is easy to calculate what the expected <sup>15</sup>N and <sup>18</sup>O of the N<sub>2</sub>O produced. It would then be interesting to compare the measured values with the expected values.

Reply: We agree that it is indeed possible to estimate the predicted value of  $\delta^{15}\text{N}$  by using the accumulated product equation. An epsilon value calculated from the  $\delta^{15}\text{N-NO}_2^-$  data could be used to estimate the predicted  $\delta^{15}\text{N-N}_2\text{O}$  values, which would be different since N<sub>2</sub>O is clearly not the single product. However, for  $\delta^{18}\text{O}$  this approach would not work due to the branching effect occurring during reduction. Hereby, the O atoms get plucked off and lost along the reaction, which is also affecting the dynamics.

At the editor's discretion, and if the manuscript is not already considered too long, we would be happy to add the "predicted"  $\delta^{15}\text{N-N}_2\text{O}$  values with a short explanation.

## 1.2. Response to comments by Anonymous Referee #2

First, we would like to thank the reviewer for his/her valuable inputs and comments on our manuscript. We have to admit that the outliers in the N<sub>2</sub>O data are indeed real outliers due to a "concentration/linearity effect" during the measurement in which overly large peak areas in the raw data biased the results. After a thorough check of the raw data, these few data points were removed and the graphs were re-drawn. We contend the data now presented are valid and accurate. We apologize for the mistake.

L98: "hold the potential to disentangle abiotic and biotic NO<sub>2</sub>- reduction " - this cannot be concluded from the previous sentences, which say that for both biotic and abiotic processes we deal with significant isotope effect

Reply: We will rephrase that part.

L184: "flushed before for 5 hrs with 5.0 He" - is this right - you need to flush 5hrs? Why so long? Have you tested that this is needed?

Reply: Since we simply applied the flushing routine of the denitrifier method, the headspace vials were indeed flushed for 5 hrs. Later testing showed, that 3 hrs would also suffice. However, several hours of flushing seem to be necessary to reduce the blank value to acceptable levels, in particular when sample size is low.

L315: you mean Fig. 6 here?

Reply: We thank the reviewer for pointing this out and apologize for the mistake! Indeed, in L315 it should indeed read Fig. 6. We will change this in the manuscript!

L315: Such a value seems rather not plausible, please double check your measurements and check how reliable is this value. There is no known process which could result in such negative value. Similarly, in 6C - I'd even doubt the value of -40 permil, unless you have ideas to explain this.

Reply: As already mentioned, we carefully checked the raw data as well as the corrected data files again and we have to admit that these values are indeed outliers caused by very high peak areas (concentration effect). We corrected the graphs accordingly (see graph attached).

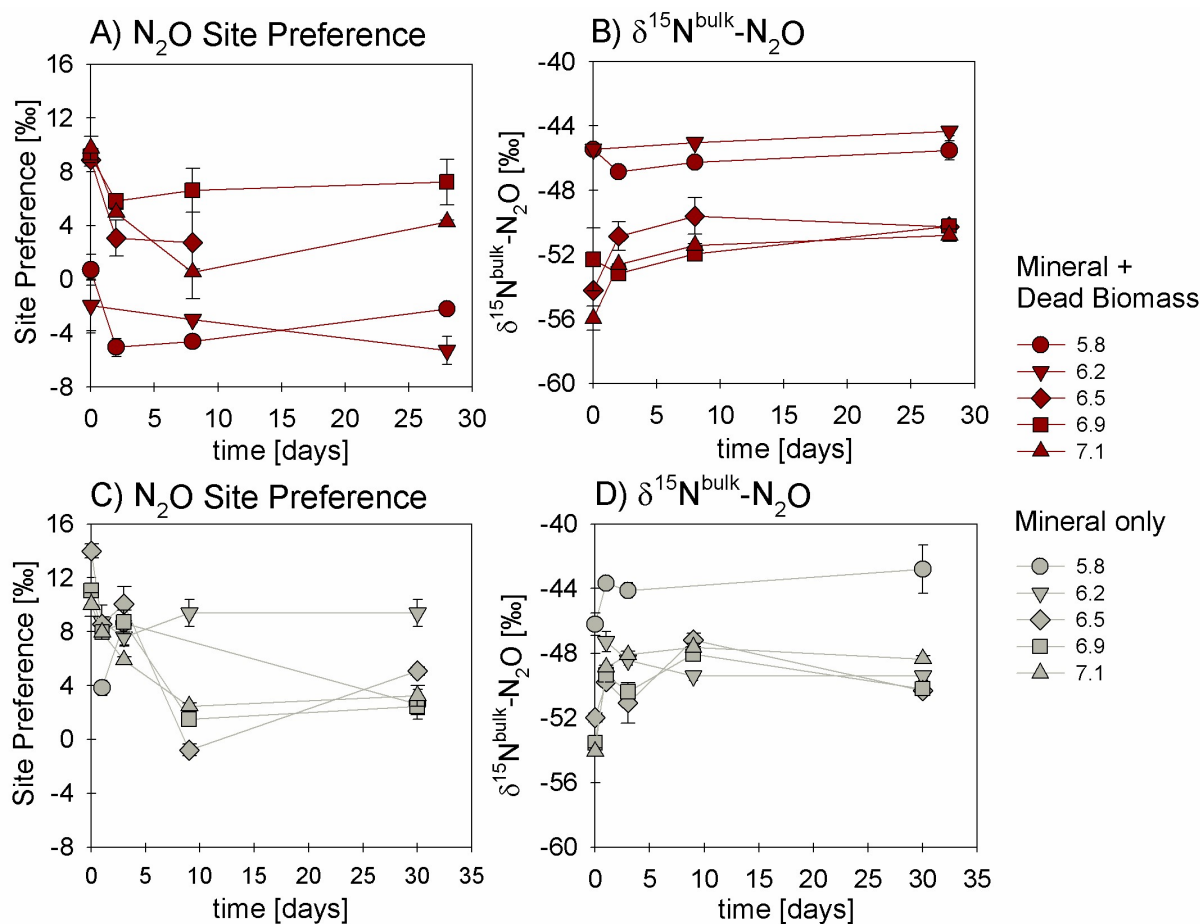


Figure 3: Same as Figure 2 - Site Preference (SP; A, C) and  $\delta^{15}\text{N}^{\text{bulk}}-\text{N}_2\text{O}$  (B, D) values of  $\text{N}_2\text{O}$  produced in experiments amended with mineral + dead biomass (red) and mineral-only (grey)

L346: Is further  $\text{N}_2\text{O}$  reduction to  $\text{N}_2$  also possible? If not, please explain why.

Reply: Considering previous publications (Rivallan et al., 2009; Doane, 2017; Phillips et al, 2016), an abiotic reduction of  $\text{N}_2\text{O}$  to  $\text{N}_2$  is indeed possible, particularly in the presence of a reactive surface.

See L559-570: “Abiotic decomposition of  $\text{N}_2\text{O}$  to  $\text{N}_2$  in the presence of Fe-bearing zeolites has been investigated previously (Rivallan et al., 2009). However, it remains unclear if this process could also occur here. Fractional  $\text{N}_2\text{O}$  reduction is also not explicitly indicated by the SP values, which would reflect an increase with  $\text{N}_2\text{O}$  reduction (Ostrom et al., 2007; Winther et al., 2018) [...] However, since  $\text{N}_2\text{O}$  concentrations, even if minor, are increasing towards the end of the experiments, production and possible decomposition as well as ongoing sorption mechanisms might also serve as possible explanation leading to these rather low SP values.”

However, with regards to the rather low  $\text{N}_2\text{O}$  concentrations and given the relatively constant  $\delta^{15}\text{N}^{\text{bulk}}-\text{N}_2\text{O}$  values, abiotic  $\text{N}_2$  production seems plausible. First, the  $\text{N}_2\text{O}$  produced here accounts only for  $\sim 0.7\%$  of the total  $\text{NO}_2^-$  reduced in the experiments. This large difference might be caused by sorption processes or simply by the fact that  $\text{N}_2\text{O}$  is not the final product (Note: accumulation of the intermediates e.g.  $\text{NO}$ , is quite unlikely since they are extremely reactive). Furthermore, if  $\text{N}_2\text{O}$  were indeed the final and only product, its  $\delta^{15}\text{N}^{\text{bulk}}$  values should approximate the  $\delta^{15}\text{N}-\text{NO}_2^-$  values (starting off lighter than  $\delta^{15}\text{N}-\text{NO}_2^-$  and increasing over incubation time). However, here the  $\delta^{15}\text{N}^{\text{bulk}}-\text{N}_2\text{O}$  values remained relatively steady or did not increase much throughout the experiment, which might indicate that  $\text{N}_2\text{O}$  is not just produced but possibly also further reduced (multistep-reaction). Therefore, the production of  $\text{N}_2$ , although abiotic, seems quite likely. We clarify this in the revised MS.



As written in L597-601: “Considering that the N<sub>2</sub>O concentrations measured in our experiments were comparatively low and that  $\delta^{15}\text{N}^{\text{bulk}}\text{-N}_2\text{O}$  values did not noticeably change throughout the experiments, formation of N<sub>2</sub> via abiotic interactions between NO<sub>2</sub><sup>-</sup> and NO may also be involved (Doane, 2017; Phillips et al., 2016). Hence, N<sub>2</sub>O is possibly involved in the reaction either as an intermediate or as a side product, and can thereby influence the overall N and O isotope dynamics.”.

L484: This is not clear:  $\delta^{15}\text{N}$  decrease and initial decrease?

Reply: Here, we meant the decrease in  $\delta^{15}\text{N}$  and an observed initial decrease in the concentration of NO<sub>2</sub><sup>-</sup>. We will add “concentration” to avoid further confusion.

L547: "was calculated is based" - sentence to be rewritten

Reply: Again, we thank the reviewer for reading our manuscript so carefully. This will of course be corrected.

L548: What do the arrows mean? (in table 3)

Reply: The arrows were added to indicate an overall increase (↑) or decrease (↓) from the initial delta value. We will correct a mistake (line for  $\delta^{15}\text{N}\text{-NO}_2^-$  values - arrow for DB + mineral setup should point up) that we only now detected, and we will add the explanation in the caption of the table.

L614: This last sentence is not stated in the discussion - in discussion you just say it is unsure if abiotic N<sub>2</sub> production is possible. Please explain this more detailed.

It is not said in the discussion what is the isotope effect of abiotic N<sub>2</sub>O reduction to N<sub>2</sub> (is this known?) - so I do not understand how N<sub>2</sub>O isotopic results can suggest its occurrence.

Reply: Generally, N<sub>2</sub> production is still assumed to be caused mainly by enzymatic reactions. However, there are studies providing evidence for abiotic N<sub>2</sub> production (e.g. Rivallan et al., 2009; Phillips et al., 2016). In our manuscript, we choose to only cautiously refer to the possible abiotic N<sub>2</sub>O reduction to N<sub>2</sub>, since most N cycling studies still do not account for abiotic N<sub>2</sub> production. Furthermore, our SP values do not explicitly indicate the occurrence of fractional N<sub>2</sub>O reduction (N<sub>2</sub>O accumulates, SP values remain rather steady). Unfortunately, we did not analyse N<sub>2</sub> samples, hence we do not know the range of N<sub>2</sub> concentrations and/or isotope values, which would help to better address this aspect.

To the best of our knowledge, the isotope effect of abiotic N<sub>2</sub>O reduction to N<sub>2</sub> is unknown. As already mentioned above, N<sub>2</sub>O accumulates throughout the experiments but overall accounts only for a small fraction of the NO<sub>2</sub><sup>-</sup> reduced. Furthermore, the  $\delta^{15}\text{N}^{\text{bulk}}\text{-N}_2\text{O}$  values remained rather steady throughout the experiments, which indicates that other processes may influence the reaction dynamics and that N<sub>2</sub>O may simply be an intermediate. If, again, N<sub>2</sub>O were the final and only product,  $\delta^{15}\text{N}^{\text{bulk}}$  values would be expected to increase with decreasing NO<sub>2</sub><sup>-</sup> concentrations (and thus increasing  $\delta^{15}\text{N}\text{-NO}_2^-$ ). However,  $\delta^{15}\text{N}^{\text{bulk}}\text{-N}_2\text{O}$  values do not really change much toward the end of the experiments, and remain steady for quite some time. Thus they do not reflect the patterns expected for a final product.

## 2. List of relevant changes

### 2.1. Adjustments according to our responses to comments by anonymous Referee #1

- L147          Sampling procedure details added; “within one hour after the sample was taken via a...”
- L150          Ferrozine analysis details added; “SFA- and/or HCl-fixed samples were stored in the dark and at 4°C until”
- L153          Procedure details added; “Triplicate samples”

- L179f Procedure details added; "...upside down at room temperature and in the dark. Two nitrite isotope standards, namely (N-7373 ( $\delta^{15}\text{N}$ : -79.6‰,  $\delta^{18}\text{O}$ : +4.5‰) and N-10219 ( $\delta^{15}\text{N}$ : +2.8‰;  $\delta^{18}\text{O}$ : +88.5‰) (Casciotti & McIlvin, 2007)..."
- L182 Sentence added: "Based on replicate measurements of laboratory standards and samples, the analytical precision for  $\text{NO}_2^-$   $\delta^{15}\text{N}$  and  $\delta^{18}\text{O}$  analyses was  $\pm 0.4\%$  and  $\pm 0.6\%$  (1 SD), respectively."
- L213 Added reference to Figure S4 added (S4 – requested Figure, added to the supplementary information)
- L303 Figure 5, x-axis title changed to "ln (f)"
- L316 Figure 6 replaced with a corrected version; Caption changed to "...For pH 6.5, the final SP value (A) is missing due to analytical problems (overly large sample peak areas). Standard error calculated from biological replicates (n = 3 or 2 ) is represented by the error bars."
- L321-327 References to Figures S5 and S6 changed to S6 and S7, respectively
- L598ff Changed to "Considering that the  $\text{N}_2\text{O}$  concentrations measured in our experiments were comparatively low and that  $\delta^{15}\text{N}^{\text{bulk}}\text{-N}_2\text{O}$  values did not noticeably change throughout the experiments, it is **unlikely that  $\text{N}_2\text{O}$  is the final product**, and formation of  $\text{N}_2$  via abiotic interactions between  $\text{NO}_2^-$  and  $\text{NO}$  is probably also involved (Doane, 2017; Phillips et al., 2016). Indeed, if **accumulated as the final product, the  $\delta^{15}\text{N}^{\text{bulk}}\text{-N}_2\text{O}$  value at the end of the incubation should be  $\sim 33\%$  (according to closed-system accumulated-product Rayleigh dynamics), significantly higher than what we measured ( $\sim -50 \pm 6 \%$ )**. Hence, whether  $\text{N}_2\text{O}$  is an intermediate or parallel side product, its role in the overall reaction complicates N and O isotope mass balance dynamics in complex ways."

## 2.2. Adjustments according to our responses to comments by anonymous Referee #2

- L98-100 "This suggests that coupled N and O isotope measurements hold the potential to disentangle abiotic and biotic  $\text{NO}_2^-$  reduction in the presence of Fe(II)." changed to "However, reaction kinetics can significantly affect isotope reaction dynamics, and chemodenitrification is possibly impacted by e.g. concentration effects and/or the presence of different catalysts (i.e. surfaces, organics). Hence, performing coupled N and O isotope measurements might help to gain deeper insights into the mechanistic details and fractionation systematics of  $\text{NO}_2^-$  reduction in the presence of Fe(II)."
- L315 "(Figure 5 A,C)" replaced by "(Figure 6 A, C)"
- L316 Figure 6 replaced with a corrected version; Caption changed to "...For pH 6.5, the final SP value (A) is missing due to analytical problems (overly large sample peak areas). Standard error calculated from biological replicates (n = 3 or 2 ) is represented by the error bars."
- L484f "...was observed with the initial decrease..." changed to "...occurred in parallel contemporaneously with initially decreasing in  $\text{NO}_2^-$  concentrations."
- L545ff Table 3 – Caption corrected (plus values): " $\delta^{15}\text{N}$  and  $\delta^{18}\text{O}$  values were calculated using  $\bar{x}_{t0} - \bar{x}_{tend}$ . Isotope fractionation was calculated is based on the slope between the lowest initial value (here at t1) and tend for all pH." changed to " $\delta^{15}\text{N}$  and  $\delta^{18}\text{O}$  values were calculated using  $\bar{x}_{t0} - \bar{x}_{tend}$ , whereas an overall increase from the initial value is marked with  $\uparrow$ , and a decrease with  $\downarrow$ . The calculated isotope fractionation factor ( $\epsilon$ ) is based on the slope between the lowest initial value (here at  $t_1$ ) and  $t_{end}$  for all pH."



L598ff Changed to “Considering that the N<sub>2</sub>O concentrations measured in our experiments were comparatively low and that  $\delta^{15}\text{N}^{\text{bulk}}\text{-N}_2\text{O}$  values did not noticeably change throughout the experiments, **it is unlikely that N<sub>2</sub>O is the final product, and formation of N<sub>2</sub> via abiotic interactions between NO<sub>2</sub><sup>-</sup> and NO is probably also involved** (Doane, 2017; Phillips et al., 2016). Indeed, if accumulated as the final product, the  $\delta^{15}\text{N}^{\text{bulk}}\text{-N}_2\text{O}$  value at the end of the incubation should be  $\sim 33\%$  (according to closed-system accumulated-product Rayleigh dynamics), significantly higher than what we measured ( $\sim -50 \pm 6 \%$ ). Hence, whether N<sub>2</sub>O is an intermediate or parallel side product, its role in the overall reaction complicates N and O isotope mass balance dynamics in complex ways.”

### 2.3. Adjustments according to the editors' recommendations

L62 “EPS has [...] electron shuttles” changed to EPS have [...] electron shuttles”  
L132 “[...] 25 min at 4000 rpm (Eppendorf, 5430 R).” changed to “[...] 3956.6 × g (4000 rpm; Eppendorf, 5430 R, Rotor F-35-6-30).”  
L142 “[...] (13400 rpm; Eppendorf, MiniSpin).” changed to “[...] (12100 × g/ 13400 rpm; Eppendorf, MiniSpin).”  
L201 “[...] the enthalpies [...]” changed to “[...] electrochemical potentials [...]”  
L202 “[...], standard enthalpy values” changed to “[...], standard electrode potentials”

### 2.4. General Adjustments

L48 L55 to 65 moved upwards, removed L48 to L50  
L50f Sentence merged with first part of the next sentence  
L53 Added “EPS has been demonstrated to...”  
L55 “biologically” changed to “enzymatically”  
L70 Reference added (Zhu-Barker et al., 2012)  
L203 Figure 1: Caption corrected – pH 5.8  
L235 “lost” changed to “processing failed”  
L251 Added “sample processing failed for the”, removed “was lost”  
L291 Added reference to Figure 4 C  
L295 (Figure S4) Rayleigh plot for mineral only experiments now added to Supplementary information file  
L309 “amended” replaced with “mineral plus DB”; “(SP)” added after “Site preference”  
L314f SP values in text replaced with corrected values  
L356-358 Sentence deleted  
L451-454 Sentence deleted  
L532 “...(abiotic  $-46.5 \pm 0.2\%$ ; dead biomass  $-49.4 \pm 1.0\%$ )...” changed to “...(abiotic  $-49.5 \pm 0.6\%$ ; dead biomass  $-50.5 \pm 0.8\%$ )...”  
L555 “mineral-only treatment (27.9%) is only slightly higher than that of the DB experiment (23.2%),” changed to “mineral-only treatment (30.9%) is slightly higher than that of the DB experiment (24.4%)”  
L562f “relatively low ( $6.0 \pm 0.8\%$ ;  $1.7 \pm 1.2\%$ ; Fig. 6) “ changed to “relatively low ( $6.5 \pm 0.8\%$ ;  $2.3 \pm 1.2\%$ ; Fig. 6, Table 3).”  
L602 Figure 8 slightly corrected (colours of bonds between species)

- L661-664 Acknowledgements corrected (added: Toby Samuels and Louis Rees)
- L675ff Changed formatting of the reference list
- Supplements S4 to S7 were corrected (L20: now S4 – graph depicting N<sub>2</sub>O versus NO<sub>2</sub><sup>-</sup> concentrations, requested by referee#1; L24 now S5 – Rayleigh plots for the mineral-only setups; L29: now S6 – Rayleigh plots for N<sub>2</sub>O δ<sup>15</sup>N<sup>α</sup>, δ<sup>15</sup>N<sup>bulk</sup> and site preference, SP; L34: now S7 – Plot showing δ<sup>18</sup>O vs δ<sup>15</sup>N<sup>bulk</sup> in N<sub>2</sub>O for mineral-only and mineral plus dead biomass setups)

# 1 Impact of reactive surfaces on the abiotic reaction between nitrite and 2 ferrous iron and associated nitrogen and oxygen isotope dynamics

3 Anna-Neva Visser<sup>1,4</sup>, Scott D. Wankel<sup>2</sup>, Pascal A. Niklaus<sup>3</sup>, James M. Byrne<sup>4</sup>, Andreas A. Kappler<sup>4</sup>,  
4 Moritz F. Lehmann<sup>1</sup>

5 <sup>1</sup>Department of Environmental Sciences, Basel University, Bernoullistrasse 30, 4056 Basel, Switzerland

6 <sup>2</sup>Woods Hole Oceanographic Institution, Woods Hole, 360 Woods Hole Rd, MA 02543, USA

7 <sup>3</sup>Department of Evolutionary Biology and Environmental Studies, University of Zürich, Winterthurerstrasse 190, 8057 Zürich,  
8 Switzerland

9 <sup>4</sup>Department of Geosciences, Tübingen University, Hölderlinstrasse 12, 72074 Tübingen, Germany

10 Correspondence to: Anna-Neva Visser (a.visser@unibas.ch)

11 **Abstract.** Anaerobic nitrate-dependent Fe(II) oxidation (NDFeO) is widespread in various aquatic environments, and plays a  
12 major role in iron and nitrogen redox dynamics. However, evidence for truly enzymatic, autotrophic NDFeO remains limited,  
13 with alternative explanations involving coupling of heterotrophic denitrification with abiotic oxidation of structurally-bound  
14 or aqueous Fe(II) by reactive intermediate N species (chemodenitrification). The extent to which chemodenitrification is  
15 caused, or enhanced, by *ex vivo* surface catalytic effects has, so far, not been directly tested. To determine whether the presence  
16 of either a Fe(II)-bearing mineral or dead biomass (DB) catalyses chemodenitrification, two different sets of anoxic batch  
17 experiments were conducted: 2 mM Fe(II) was added to a low-phosphate medium, resulting in the precipitation of vivianite  
18 ( $\text{Fe}_3(\text{PO}_4)_2$ ), to which later 2 mM nitrite ( $\text{NO}_2^-$ ) was added, with or without an autoclaved cell suspension ( $\sim 1.96 \times 10^8$  cells  $\text{ml}^{-1}$ )  
19 of *Shewanella oneidensis* MR-1. Concentrations of nitrite, nitrous oxide ( $\text{N}_2\text{O}$ ) and iron ( $\text{Fe}^{2+}$ ,  $\text{Fe}_{\text{tot}}$ ) were monitored over  
20 time in both setups to assess the impact of Fe(II) minerals and/or DB as catalysts of chemodenitrification. In addition, the  
21 natural-abundance isotope ratios of  $\text{NO}_2^-$  and  $\text{N}_2\text{O}$  ( $\delta^{15}\text{N}$  and  $\delta^{18}\text{O}$ ) were analysed to constrain associated isotope effects. Up  
22 to 90% of the Fe(II) was oxidized in the presence of DB, while only ~65% were oxidized under mineral-only conditions,  
23 suggesting an overall lower reactivity of the mineral-only setup. Similarly, the average  $\text{NO}_2^-$  reduction rate in the mineral-only  
24 experiments ( $0.004 \pm 0.003$   $\text{mmol L}^{-1} \text{day}^{-1}$ ) was much lower compared to experiments with mineral plus DB ( $0.053 \pm 0.013$   
25  $\text{mmol L}^{-1} \text{day}^{-1}$ ), as was  $\text{N}_2\text{O}$  production ( $204.02 \pm 60.29$   $\text{nmol/L*day}$ ). The  $\text{N}_2\text{O}$  yield per mole  $\text{NO}_2^-$  reduced was higher in  
26 the mineral-only setups (4%) compared to the experiments with DB (1%), suggesting the catalysis-dependent differential  
27 formation of NO. N- $\text{NO}_2^-$  isotope ratio measurements indicated a clear difference between both experimental conditions: In  
28 contrast to the marked  $^{15}\text{N}$  isotope enrichment during active  $\text{NO}_2^-$  reduction ( $^{15}\epsilon_{\text{NO}_2} = +10.3\%$ ) observed in the presence of  
29 DB,  $\text{NO}_2^-$  loss in the mineral-only experiments exhibited only a small N isotope effect ( $< +1\%$ ). The  $\text{NO}_2^-$ -O isotope effect  
30 was very low in both setups ( $^{18}\epsilon_{\text{NO}_2} < 1\%$ ), most likely due to substantial O isotope exchange with ambient water. Moreover,  
31 during the low-turnover conditions (i.e.; in the mineral-only experiments, as well as initially in experiments with DB), the  
32 observed  $\text{NO}_2^-$  isotope systematics suggest, transiently, a small inverse isotope effect (i.e.; decreasing nitrite  $\delta^{15}\text{N}$  and  $\delta^{18}\text{O}$ )

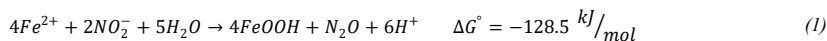
33 with decreasing concentrations), possibly related to transitory surface complexation mechanisms. Site preference (SP) of the  
34 <sup>15</sup>N isotopes in the linear N<sub>2</sub>O molecule for both setups ranged between 0 to 14‰, notably lower than previously reported for  
35 chemodenitrification. Our results imply that chemodenitrification is dependent on the available reactive surfaces, and that the  
36 NO<sub>2</sub><sup>-</sup> (rather than the N<sub>2</sub>O) isotope signatures may be useful for distinguishing between chemodenitrification catalysed by  
37 minerals, chemodenitrification catalysed by dead microbial biomass, and possibly true enzymatic NDFeO.

## 38 1. Introduction

39 Iron (Fe) is essential for all living beings and its biogeochemical cycling has been studied extensively (Expert, 2012; Lovley,  
40 1997). Although Fe is ubiquitous in most environments, it is not always bioavailable (Andrews et al., 2003; Ilbert and  
41 Bonnefoy, 2013), and microorganisms must often cope with Fe limitation in their respective environments (Braun and Hantke,  
42 2013; Ilbert and Bonnefoy, 2013). This is especially true at circumneutral pH and oxic conditions, where Fe(II) is quickly  
43 oxidized by O<sub>2</sub> and thus only present as poorly soluble Fe(III)(oxyhydr)oxides (Cornell and Schwertmann, 2003; Stumm and  
44 Sulzberger, 1992). In contrast, under anoxic conditions, Fe is mainly present as either dissolved Fe<sup>2+</sup> or as mineral-bound Fe(II)  
45 in ~~iron-Fe~~ phosphates or carbonates (Charlet et al., 1990; Luna-Zaragoza et al., 2009). Here, microbes use electron acceptors  
46 other than O<sub>2</sub> for respiration (He et al., 2016; Lovley, 2012; Straub et al., 1996). One redox pair that has been proposed to be  
47 exploited by microbes under anoxic conditions is NO<sub>3</sub><sup>-</sup>/Fe<sup>2+</sup>, through a mechanism known as nitrate-dependent Fe(II) oxidation  
48 (NDFeO) (Ilbert and Bonnefoy, 2013; Straub et al., 1996). ~~To date, indeed, to date, genetic evidence that clearly supports this~~  
49 ~~metabolic capacity of the studied microorganisms remains lacking (Price et al., 2018), and biogeochemical evidence is rare~~  
50 ~~and putative. The latter is mostly based on experiments with the chemolithoautotrophic culture KS, a consortium of four~~  
51 ~~different strains, including a relative of the microaerophilic *Sideroxydans/Gallionella*. This enrichment culture has been shown~~  
52 ~~to be able to oxidize Fe(II) without the addition of any organic co-substrates (Tominski et al., 2018). Tian et al. (2020)~~  
53 ~~confirmed that *Gallionellaceae* are able to perform autotrophic Fe(II)-dependent denitrification. Another more indirect line of~~  
54 ~~evidence includes results from slurry microcosm experiments with marine coastal sediments. In these experiments, Fe(II)~~  
55 ~~oxidation was still detected even after all bioavailable organics of the sediments were consumed and only NO<sub>3</sub><sup>-</sup> was left (Laufer~~  
56 ~~et al., 2016). With regards to other studies where NDFeO was initially thought to be performed by autotrophs (Chakraborty et~~  
57 ~~al., 2011; Weber et al., 2009), it was subsequently shown that the microbes rely on an organic co-substrate and must in fact be~~  
58 ~~considered mixotrophic (Klueglein et al., 2014; Muehe et al., 2009). Yet, the exact mechanism promoting NDFeO in the~~  
59 ~~microorganisms that have been investigated so far (e.g. *Acidovorax delafieldii* strain 2AN, *Pseudogulbenkiania ferrooxidans*~~  
60 ~~strain 2002) (Chakraborty et al., 2011; Weber et al., 2009), is still not fully understood. Over the past two decades, several~~  
61 ~~microorganisms have been investigated and reported to be either chemolithoautotrophic or -mixotrophic nitrate-dependent~~  
62 ~~Fe(II)-oxidising bacteria (e.g. *Acidovorax delafieldii* strain 2AN, *Pseudogulbenkiania ferrooxidans* strain 2002) (Chakraborty~~  
63 ~~et al., 2011; Weber et al., 2009). It has been suggested that extracellular electron transfer (EET) might play a major role in~~  
64 ~~NDFeO, particularly in the presence of high levels of extracellular polymeric substances (EPS) (Klueglein et al., 2014; Liu~~

Kommentiert [AV1]: Moved this part up – might improve “flow”

65 et al., 2018; Zeitvogel et al., 2017). ~~which EPS has been demonstrated to can~~ act as electron shuttles, ~~hence~~ EET may indeed  
66 provide a plausible explanation for the observed Fe(II) oxidation in these cultures (Liu et al., 2018). The existence of such an  
67 electron transfer would imply that NDFeO is not necessarily a completely ~~biologically-enzymatically~~-catalysed reaction.  
68 ~~Indeed, to date, genetic evidence that supports this metabolic capacity of the studied microorganisms remains lacking (Price~~  
69 ~~et al., 2018), and biogeochemical evidence is rare and putative. The latter is mostly based on experiments with the~~  
70 ~~chemolithoautotrophic culture KS, a consortium of four different strains, including a relative of the microaerophilic~~  
71 ~~*Sideroxydans/Gallionella*. This enrichment culture has been shown to be able to oxidize Fe(II) without the addition of any~~  
72 ~~organic co-substrates (Tominski et al., 2018). Tian et al. (2020) confirmed that *Gallionellaceae* are able to perform autotrophic~~  
73 ~~Fe(II)-dependent denitrification. Another more indirect line of evidence includes results from slurry microcosm experiments~~  
74 ~~with marine coastal sediments. In these experiments, Fe(II) oxidation was still detected even after all organics of the sediments~~  
75 ~~were consumed and only nitrate was left (Laufer et al., 2016). With regards to other studies where NDFeO was initially thought~~  
76 ~~to be performed by autotrophs (Chakraborty et al., 2011; Weber et al., 2009), it was subsequently shown that the microbes rely~~  
77 ~~on an organic co-substrate and must in fact be considered mixotrophic (Klueglein et al., 2014; Muehe et al., 2009). Yet, the~~  
78 ~~exact mechanism promoting NDFeO is still not fully understood. Considering that all putative NDFeO strains were grown~~  
79 under high (up to 10 mM) nitrate (NO<sub>3</sub><sup>-</sup>) and Fe(II) concentrations, and accumulated up to several mM nitrite (NO<sub>2</sub><sup>-</sup>) from  
80 enzymatic NO<sub>3</sub><sup>-</sup> reduction, ~~it was other studies~~ suggested that the observed Fe(II) oxidation in these pure cultures may be due  
81 to the abiotic side reaction between the generated NO<sub>2</sub><sup>-</sup> and Fe(II) (Buchwald et al., 2016; Prakash Dhakal, 2013; Klueglein et  
82 al., 2014). This abiotic reaction between NO<sub>2</sub><sup>-</sup> and Fe(II) is known as chemodenitrification (Equation 1) and is proposed to  
83 lead to an enhanced production of N<sub>2</sub>O (Anderson and Levine, 1986; Buchwald et al., 2016; Zhu-Barker et al., 2015).



84 Several studies have noted that the presence of reactive surfaces may enhance the abiotic reaction (Heil et al., 2016; Sorensen  
85 and Thorling, 1991). For example, Klueglein and Kappler (2013) tested the impact of goethite on Fe-coupled  
86 chemodenitrification in the presence of high Fe(II) and NO<sub>2</sub><sup>-</sup> concentrations, and confirmed the concentration dependency of  
87 this reaction with regard to both species (Van Cleemput and Samater, 1995). Possible catalytic effects (e.g. by reactive surfaces  
88 and/or organic matter) were not tested specifically in these studies. Yet, multiple factors have been shown to affect the abiotic  
89 reaction between NO<sub>2</sub><sup>-</sup> and Fe(II) and may need to be considered (i.e.: pH, temperature, Fe<sup>2+</sup> concentrations, solubility of  
90 Fe(III)(oxyhydr)oxides, crystallinity of Fe(II) minerals, other metal ion concentrations and catalytic effects) (Van Cleemput  
91 & Samater, 1995; Klueglein & Kappler, 2013; Ottley et al., 1997). In addition, the presence of organic compounds can lead to  
92 the abiotic reduction of NO<sub>2</sub><sup>-</sup> to NO (Van Cleemput and Samater, 1995; McKnight et al., 1997; Pereira et al., 2013).  
93 Given the complex controls and potential interaction between Fe(II) and various nitrogenous compounds, including  
94 intermediates, it may be an oversimplification to state that Fe(II) oxidation observed in previous laboratory setups is solely  
95 caused by the abiotic reaction with NO<sub>2</sub><sup>-</sup>, and not, for example, stimulated by reactive surfaces (minerals, organic-detritus) or  
96 by nitric oxide (NO), a highly reactive intermediate not easily quantified in anoxic batch experiments. In order to better

97 understand the factors that may control chemodenitrification of  $\text{NO}_2^-$ , this study focuses on the possible catalytic surface effects  
98 induced by a Fe(II) mineral phase or dead biomass (DB). Furthermore, microbial cells, ~~dead biomass DB~~, or detrital waste  
99 products might not only provide additional reactive surface area, but may directly react with  $\text{NO}_2^-$  to form NO.

100 Stable isotopes of both N and O ( $\delta^{15}\text{N}$  and  $\delta^{18}\text{O}$ ) offer a promising approach to further elucidate the mechanism of NDFeO,  
101 and also to more generally expand our understanding of chemodenitrification. The N and O isotopic composition of  
102 nitrogenous compounds (e.g.,  $\text{NO}_3^-$ ,  $\text{NO}_2^-$ , and  $\text{N}_2\text{O}$ ) has been used to gain deeper insights into various N turnover processes  
103 (Granger et al., 2008; Jones et al., 2015). The dual  $\text{NO}_2^-$  (or  $\text{NO}_3^-$ ) isotope approach is based on the fact that specific N-  
104 transformation processes – biotic or abiotic – are associated with specific N and O isotope fractionation (i.e., isotope effect).  
105 In general, enzymatic processes promote the more rapid reaction of lighter N and O isotopologues, leaving the remaining  
106 substrate pool enriched in the heavier isotopes (i.e.,  $^{15}\text{N}$ ,  $^{18}\text{O}$ ) (Granger et al., 2008; Kendall & Aravena, 2000; Martin &  
107 Casciotti, 2017). Only a few studies exist that have looked into the isotope effects of chemodenitrification and reports on the  
108 associated isotope effects are variable. Consistent with what we know from biological denitrification, chemodenitrification  
109 experiments with 10 mM Fe(II) and  $\text{NO}_2^-$ , ~~with and~~ very high reaction rates, revealed a significant increase in the  $\delta^{15}\text{N}$  (up to  
110 40%) and  $\delta^{18}\text{O}$  (up to 30%)  $\text{NO}_2^-$  values, corresponding to an overall N and O isotope effect of  $^{15}\epsilon$   $18.1 \pm 1.7\%$  and  $^{18}\epsilon$   $9.8 \pm$   
111  $1.8\%$ , as well as a  $\Delta^{15}\text{N}$  (i.e., the difference between  $\delta^{15}\text{NO}_2^-$  and  $\delta^{15}\text{N}_2\text{O}$ ) of  $27 \pm 4.5\%$  (Jones et al., 2015). ~~However, since~~  
112 ~~reaction kinetics are able to meddle with the can~~ significantly affect isotope reaction dynamics, and chemodenitrification is  
113 ~~possibly impacted by e.g. the concentration effect~~ concentration effects and/or the presence of different catalysts (i.e. surfaces,  
114 ~~organics). Hence, performing This suggests that~~ coupled N and O isotope measurements ~~might help to gain deeper insights~~  
115 ~~into the mechanistic details and fractionation dynamics-systematics of hold the potential to disentangle abiotic and biotic~~  $\text{NO}_2^-$   
116 reduction in the presence of Fe(II). Here, in order to expand the limited dataset on the isotope effects of abiotic Fe(II)-coupled  
117 denitrification, and in turn to lay the groundwork for using  $\text{NO}_3^-/\text{NO}_2^-$  N and O isotope measurements to unravel the mechanism  
118 behind NDFeO, we studied the N and O isotope dynamics of  $\text{NO}_2^-$  reduction and  $\text{N}_2\text{O}$  production during abiotic reaction of  
119  $\text{NO}_2^-$  with Fe(II). As the extent of the formation of various Fe(III)(oxyhydr)oxides has been previously reported to enhance  
120 chemodenitrification dynamics (Chen et al., 2018; Sorensen and Thorling, 1991), we also followed mineral alteration during  
121 chemodenitrification in order to identify possible reaction patterns. A specific goal in this context was to assess the impact of  
122 Fe(II) precipitates and/or dead biomass as catalytic agents during Fe(II)-associated chemodenitrification, as well as potential  
123 mineral transformation processes associated with the abiotic oxidation of Fe(II) via reactive  $\text{NO}_x$  species.

## 124 2. Material and Methods

### 125 2.1. General experimental setup

126 For all experiments, anoxic low phosphate medium (1.03 mM  $\text{KH}_2\text{PO}_4$ , 3.42 mM NaCl, 5.61 mM  $\text{NH}_4\text{Cl}$ , 2.03 mM  $\text{MgSO}_4 \cdot 7$   
127  $\text{H}_2\text{O}$  and 0.68 mM  $\text{CaCl}_2 \cdot 2 \text{H}_2\text{O}$ , with a 7-vitamin (Widdel & Pfennig, 1981) and a SL-10 trace element solution (Widdel et  
128 al., 1983); 22 mM bicarbonate buffered) was prepared. The medium was dispensed with a Widdel flask in 1-l Schott bottles



129 and the pH for each bottle was adjusted separately by the addition of anoxic, sterile 1 M HCl. For ~~the~~ both setups, five different  
130 pH values were targeted: 5.8, 6.2, 6.5, 6.9 and 7.1. After pH adjustment, Fe(II)Cl<sub>2</sub> was added to reach a concentration of ~2  
131 mM Fe(II), and, if necessary, the pH was re-adjusted. The medium was kept for 48 h at 4°C, resulting in amorphous, green-  
132 greyish Fe(II) precipitates. In addition, ~2 mM NaNO<sub>2</sub> and ~1 mM Na-acetate were added to the main medium stocks shortly  
133 before 10 ml aliquots of the medium were distributed into 20 ml headspace vials (heat-sterilized) in an anoxic glove box  
134 (MBraun, N<sub>2</sub>, 100%). Acetate was added to mimic experiments, in which bacteria are cultivated (yet, acetate concentrations  
135 did not change during incubations, underscoring that the organic acid was not involved in the observed reactions; data not  
136 shown). All headspace vials were closed with black butyl stoppers and crimp-sealed [headspace N<sub>2</sub>/CO<sub>2</sub> (90/10, v/v)]. All vials  
137 were then incubated at 28°C in the dark.

138 *Incubations with dead-biomass* – *Shewanella oneidensis* MR-1, a ~~facultatively~~ ~~facultative~~ aerobic Gram-negative bacterium, is  
139 seen as model organism for bioremediation studies due to its various respiratory abilities (Heidelberg et al., 2002; Lies et al.,  
140 2005). It is known to perform dissimilatory metal reduction by utilizing alternative terminal electron acceptors such as  
141 elemental sulfur, Mn(IV), Fe(III) or NO<sub>3</sub><sup>-</sup>. Since *S. oneidensis* produces large amounts of EPS (Dai et al., 2016; Heidelberg et  
142 al., 2002), but is not capable of oxidizing Fe(II) (Lies et al., 2005; Piepenbrock et al., 2011) (i.e. no interference with abiotic  
143 reactions involving Fe/chemodenitrification), we chose concentrated and sterilized *S. oneidensis* for our dead-biomass  
144 experiments. In preparation of these experiments, *S. oneidensis* MR-1 was grown oxically on a LB (lysogeny broth) medium  
145 (10 g tryptone, 5 g yeast extract, 10 g NaCl in 1 l DI water) in six 250 ml Erlenmeyer flasks. After 12 hrs, cultures were  
146 transferred into 50 ml Falcon tubes and centrifuged for 25 min at ~~3956.6 × g 4000 rpm~~ (4000 rpm, Eppendorf, 5430 R, Rotor  
147 F-35-6-30). Cell-containing pellets were washed twice with oxalic acid and centrifuged again, followed by three more washing  
148 steps with TRIS buffer prior to final resuspension in 5 ml TRIS buffer. Pellet suspensions were pooled in a 100 ml serum bottle  
149 and autoclaved twice to ensure that all cells were killed. Before distribution of the medium into 20 ml vials (see above), cell  
150 suspension was added to yield a cell density of ~1.96×10<sup>8</sup> cell ml<sup>-1</sup>. Care was taken to ensure the homogenous distribution of  
151 mineral precipitates and the dead biomass.

## 152 2.2. Sampling and sample preparation

153 Incubations were run for approximately 30 days, and sampling was performed in an anoxic glove box (MBraun, N<sub>2</sub>, 100%) at  
154 five time points. For each time point, and for each pH treatment, 9 replicates were prepared. Therefore, variations between the  
155 replicates and the different sampling time points are possible. For sampling, the headspace was quantitatively transferred into  
156 12 ml He-purged Exetainer vials (LABCO) for N<sub>2</sub>O concentration measurements. Then, 2 ml of the liquid sample were  
157 transferred into 2 ml Eppendorf tubes, centrifuged for 5 min (12100 × g /13400 rpm; Eppendorf, MiniSpin), followed by a  
158 1:10 dilution of the supernatant in 1 ml anoxic MilliQ water for NO<sub>2</sub><sup>-</sup> quantification. A second 100 µl aliquot was diluted 1:10  
159 in 40 mM sulfamic acid (SFA) for iron determination by ferrozine analysis (Granger and Sigman, 2009; Klueglein and Kappler,  
160 2013). The remaining supernatant was used for HPLC and NO<sub>2</sub><sup>-</sup> isotope analysis. Finally, the spun-down pellet was

161 resuspended in 1 M HCl for ferrozine analysis (Stookey, 1970). All liquid samples were stored at 4°C in the dark until further  
162 processing. The remaining liquid samples were used for <sup>57</sup>Fe Mössbauer spectroscopy.

### 163 2.3. Analytical techniques

164 *NO<sub>2</sub><sup>-</sup> concentrations* – NO<sub>2</sub><sup>-</sup> concentrations were quantified within one hour after the sample was taken via using a standard  
165 segmented continuous-flow analytical (CFA, SEAL Analytics) photometric techniques (Snyder and Adler, 1976). NO<sub>2</sub><sup>-</sup>  
166 reduction rates were calculated based on the observed net concentration decrease ( $\overline{[C]}_{t_0} - \overline{[C]}_{t_{end}} \pm \text{standard error}$ ) with time.

167 *Fe concentrations* – SFA- and/or HCl-fixed samples were stored in the dark and at 4°C until Fe(II) concentrations was/were  
168 analysed using the ferrozine assay (Stookey, 1970), which was adapted for NO<sub>2</sub><sup>-</sup>-containing samples by Klueglein et al. (2013).  
169 Total Fe(II) concentrations were calculated as the sum of the  $Fe_{aq}^{2+} + Fe(II)_{pellet}$  concentrations.

170 *N<sub>2</sub>O concentrations* – Prior to the quantification of the N<sub>2</sub>O, the sample gas was diluted (1:5) with 5.0 He. The samples  
171 T(triplicate samples) were then analysed using a gas chromatograph with an electron capture detector (GC-ECD; Agilent  
172 7890 with micro-ECD and FID; Porapak Q 80/100 column). GC-ECD measurements were calibrated using four standard gases  
173 containing different concentrations of N<sub>2</sub>O (Niklaus et al., 2016). N<sub>2</sub>O production rates were calculated based on the observed  
174 net N<sub>2</sub>O concentration increase ( $\overline{[C]}_{t_{end}} - \overline{[C]}_{t_0} \pm \text{standard error}$ ) with time.

175 *<sup>57</sup>Fe Mössbauer spectroscopy* - For Mössbauer spectroscopic analyses, the remaining liquid samples (ca. 8 ml) were processed  
176 inside an anoxic glove box. The entire liquid including the precipitates was passed through a 0.45 µm filter. The wet filter was  
177 then sealed between two layers of Kapton tape and kept inside sealed Schott bottles in a freezer (-20°C) under anoxic conditions  
178 until analysis. From the treatments with DB, samples were collected at day 0 at pH 6.8 and at the end of the experiment (~30  
179 days) for pH 6.8 and 5.8. For the mineral-only experiment, only one sample (time point zero, pH 6.8) was analysed, as a basis  
180 for comparison with the DB experiments (i.e., to verify whether DB has an immediate effect on the mineral phase). Taking  
181 care to minimize exposure to air, samples were transferred from the air-tight Schott bottles and loaded inside a closed-cycle  
182 exchange gas cryostat (Janis cryogenics). Measurements were performed at 77 K with a constant acceleration drive system  
183 (WissEL) in transmission mode with a <sup>57</sup>Co/Rh source and calibrated against a 7µm thick α-<sup>57</sup>Fe foil measured at room  
184 temperature. All spectra were analysed using Recoil (University of Ottawa) by applying a Voight Based Fitting (VBF) routine  
185 (Lagarec and Rancourt, 1997; Rancourt and Ping, 1991). The half-width at half maximum (HWHM) was fixed to a value of  
186 0.130 mm/s during fitting.

187 *Nitrite N and O isotope measurements* – The nitrogen (N) and oxygen (O) isotope composition of NO<sub>2</sub><sup>-</sup> was determined using  
188 the azide method (McIlvin and Altabet, 2005). This method is based on the chemical conversion of NO<sub>2</sub><sup>-</sup> to gaseous N<sub>2</sub>O at a  
189 low pH (4 to 4.5) (McIlvin and Altabet, 2005), and the subsequent analysis of the concentrated and purified N<sub>2</sub>O by gas  
190 chromatography— isotope ratio mass spectrometry (GC-IRMS). Addition of 0.6 M NaCl to the acetic acid-azide solution was  
191 conducted in order to minimize oxygen isotope exchange (McIlvin and Altabet, 2005). The acetic acid-azide solution was  
192 prepared freshly every day (McIlvin and Altabet, 2005) and kept in a crimp sealed (grey butyl stopper) 50 ml serum bottle.

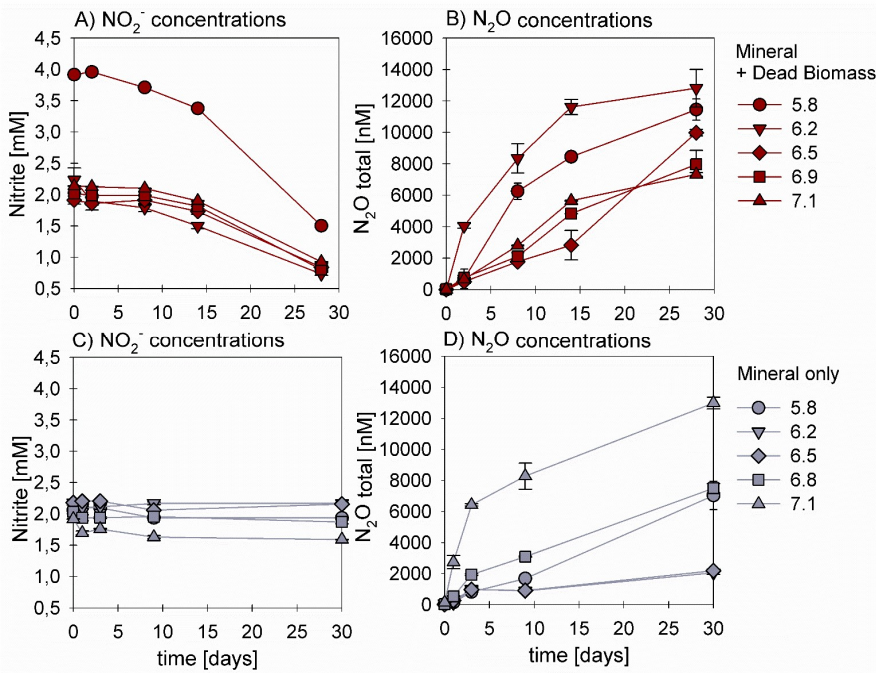
193 Sample volume equivalent to 40 nmol NO<sub>2</sub><sup>-</sup> was added to pre-combusted headspace vials, filled up to 3 ml with anoxic MilliQ  
194 water, and crimp-sealed. Then, 100 µl of the acetic acid/azide solution was added. After ~7 hrs, 100 µl of 6 M NaOH was  
195 added to stop the reaction. Until isotope analysis by a modified purge and trap gas bench coupled to CF-IRMS (McIlvin and  
196 Casciotti, 2010), the samples were stored upside down at room temperature and in the dark. Two nNitrite isotope standards,  
197 namely-(N-7373 ( $\delta^{15}\text{N}$ : -79.6‰,  $\delta^{18}\text{O}$ : +4.5‰) and N-10219 ( $\delta^{15}\text{N}$ : +2.8‰;  $\delta^{18}\text{O}$ : +88.5‰)(Casciotti & McIlvin, 2007), were  
198 prepared on the day of isotope analysis and processed the same way as samples. N and O isotope data are expressed in the  
199 common  $\delta$  notation and reported as per-mille deviation (‰) relative to AIR N<sub>2</sub> and VSMOW, respectively ( $\delta^{15}\text{N} = ([^{15}\text{N}]/[^{14}\text{N}]_{\text{sample}} / [^{15}\text{N}]/[^{14}\text{N}]_{\text{air-N}_2} - 1) \times 1000\text{‰}$  and  $\delta^{18}\text{O} = ([^{18}\text{O}]/[^{16}\text{O}]_{\text{sample}} / [^{18}\text{O}]/[^{16}\text{O}]_{\text{VSMOW}} - 1) \times 1000\text{‰}$ ). Based on replicate  
200 measurements of laboratory standards and samples, the analytical precision for NO<sub>2</sub><sup>-</sup>  $\delta^{15}\text{N}$  and  $\delta^{18}\text{O}$  analyses was  $\pm 0.4\text{‰}$  and  
201  $\pm 0.6\text{‰}$  (1 SD), respectively.  
202  
203 *N<sub>2</sub>O N and O isotope measurements* – Triplicate 12 nmol samples of N<sub>2</sub>O were injected into 20 ml headspace vials that were  
204 flushed before for 5 hrs with 5.0 He (injection volumes according to the N<sub>2</sub>O concentrations determined before). The N<sub>2</sub>O was  
205 then analysed directly using CF-IRMS (see above). Two standard gases with known  $\delta^{15}\text{N}$  and  $\delta^{18}\text{O}$  values were analysed along  
206 with the samples, namely FLCA06261 ( $\delta^{15}\text{N}$ : -35.74‰,  $\delta^{15}\text{N}^{\alpha}$ : -22.21‰,  $\delta^{15}\text{N}^{\beta}$ : -49.28‰,  $\delta^{18}\text{O}$ : 26.94‰) and FL53504 ( $\delta^{15}\text{N}$ :  
207 48.09‰,  $\delta^{15}\text{N}^{\alpha}$ : 1.71‰,  $\delta^{15}\text{N}^{\beta}$ : 94.44‰,  $\delta^{18}\text{O}$ : 36.01‰) (provided by J. Mohn, EMPA; e.g. Mohn et al., 2014). The gases  
208 were calibrated on the Tokyo Institute of Technology scale for bulk and site-specific isotopic composition (Ostrom et al., 2018;  
209 Sakae Toyoda et al., 1999). Ratios of m/z 45/44, 46/44 and the 31/30 signals were used to calculate values of  $\delta^{15}\text{N}^{\text{bulk}}$   
210 (referenced against AIR-N<sub>2</sub>),  $\delta^{18}\text{O}$  (referenced against V-SMOW), and site-specific  $\delta^{15}\text{N}^{\alpha}$ ,  $\delta^{15}\text{N}^{\beta}$  based on Frame and Casciotti  
211 (2010). Site preference (SP) was calculated as  $\delta^{15}\text{N}^{\alpha} - \delta^{15}\text{N}^{\beta}$  (Sutka et al., 2006; Toyoda and Yoshida, 1999).

#### 212 2.4. Pourbaix diagram

213 In order to predict the stability and behaviour of the N- and Fe(II)-bearing chemical species in the same system, a Pourbaix  
214 (Eh-pH) diagram was constructed (Delahay et al., 1950) as a valuable tool to predict possible reactions and speciation of end  
215 products under different experimental conditions. To calculate the electrochemical potentials the enthalpies for the stepwise  
216 reduction of nitrite during denitrification, as well as Fe(II) oxidation reactions, standard electrode potentials enthalpy values  
217 were taken from different references (Table S1). The Pourbaix diagram presented in the discussion was devised using  
218 concentrations measured during the experiments performed for this study.

219 3. Results

220 3.1. Chemodenitrification kinetics

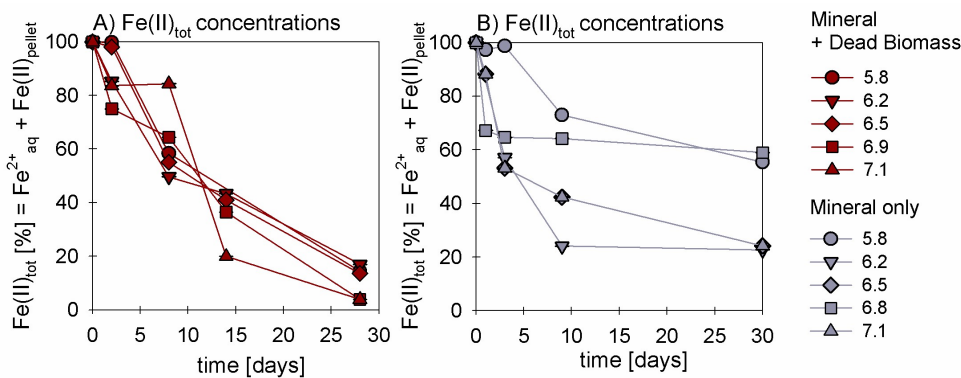


221  
 222 **Figure 1: Nitrite reduction (A, C) and N<sub>2</sub>O production (B, D) over time in the mineral + dead biomass (red) and mineral-only (grey)**  
 223 **setups over time and at different pH. Please note that at pH 5.8 twice the amount of nitrite was accidentally introduced. Standard**  
 224 **error calculated from biological replicates (n = 9) is represented by the error bars.**

225 In the presence of DB, NO<sub>2</sub><sup>-</sup> reduction rates were much higher compared to the mineral-only setup (Figure 1 A, C), with up to  
 226 ~60% of the initially amended NO<sub>2</sub><sup>-</sup> being transformed during the incubation period, independent of the pH. The addition of  
 227 DB led to a decrease in NO<sub>2</sub><sup>-</sup> concentrations from 2 mM to ~0.7 mM (Figure 1 A). The pH 5.8 treatment (unintentionally  
 228 amended with 2x NO<sub>2</sub><sup>-</sup>) also showed a similar fractional reduction. In the mineral-only setups the decrease in NO<sub>2</sub><sup>-</sup>  
 229 concentration was rather moderate and ranged between 0.3 (pH 7) and 0.1 mM (at lower pH) (Figure 1 C). In all treatments,  
 230 N<sub>2</sub>O was produced but accounted for a maximum of only 0.7% of the NO<sub>2</sub><sup>-</sup> consumed. The final N<sub>2</sub>O yield per mole NO<sub>2</sub><sup>-</sup>  
 231 reduced tended to be lower in the mineral plus DB versus the mineral-only amended setups for most of the pH (Figure 1 B vs.  
 232 D). Highest N<sub>2</sub>O production was observed at circumneutral pH (7.1) in the mineral-only setup, while maximum final N<sub>2</sub>O

233 concentrations were observed at lower pH (6.2) in the incubations with DB (Figure 1 B; S4). A systematic pH effect, however,  
 234 could not be discerned. Fe(II)<sub>total</sub> concentrations rapidly decreased in both setups. In the presence of DB, Fe(II)<sub>total</sub> oxidation  
 235 was almost complete (Figure 2A), independent of the pH, whereas in the mineral-only experiment, Fe(II)<sub>total</sub> decreased during  
 236 the first 5-10 days but then seemed to reach a steady state (Figure 2 B). At pH 6.8 and 5.8, only 40% of the Fe(II)<sub>total</sub> was  
 237 oxidized, whereas at the other pH up to 80% of the Fe(II)<sub>total</sub> initially amended was oxidized. Total Fe decreased over time  
 238 (Figure S2).

Kommentiert [AV2]: That's the additional graph requested by Ref#1



239  
 240 **Figure 2: Oxidation of total Fe(II) over time given (reported as % of initial concentration) in the mineral + dead biomass amended**  
 241 **(red)** and the mineral-only setup (grey), tested at different pH. Standard error calculated from biological replicates (n = 9) is  
 242 represented by the error bars.

243  
 244 Average rates for NO<sub>2</sub><sup>-</sup> reduction and N<sub>2</sub>O production at pH 6.8 were calculated (Table 1). Rates were calculated per day and  
 245 again these results emphasize that the amendment of dead biomass increased the rates by ~92%. Although not complete, Fe(II)  
 246 oxidation in the presence of DB was also more pronounced leading to only 10.5 ± 2.8% Fe(II) remaining compared to the  
 247 mineral-only setup in which 37.1 ± 8.2% Fe(II) remained. To complement the colorimetric data, <sup>57</sup>Fe Mössbauer spectroscopy  
 248 was performed and data are presented in detail in the next section.

249  
 250 **Table 1: Chemodenitrification kinetics and mineral transformation during mineral + dead biomass as well as the mineral only**  
 251 **experiments. T<sub>ini</sub> values represent means calculated by summarizing results across all pH ± standard error. Overall**  
 252 **reduction/production rates are calculated by subtracting [C]<sub>t0</sub> - [C]<sub>tend</sub> ± standard error / [C]<sub>tend</sub> - [C]<sub>t0</sub> ± standard error,**  
 253 **respectively and are given per day. Fe(III) values are calculated by using <sup>57</sup>Fe Mössbauer spectroscopy data. Mineral phases were**  
 254 **also identified by using <sup>57</sup>Fe Mössbauer spectroscopy with spectra collected at 77 K. Mineral-only sample taken after 28 days was**  
 255 **inadvertently destroyed prior to Mössbauer measurement.**

	Mineral + Dead Biomass	Mineral-only
NO <sub>2</sub> <sup>-</sup> reduction ( $\bar{X}$ )	0.053 ± 0.013 mmol L <sup>-1</sup> day <sup>-1</sup>	0.004 ± 0.003 mmol L <sup>-1</sup> day <sup>-1</sup>

<b>N<sub>2</sub>O production (<math>\bar{X}</math>)</b>	353.50 ±32.91 nmol L <sup>-1</sup> day <sup>-1</sup>	204.02 ±60.29 nmol L <sup>-1</sup> day <sup>-1</sup>
<b>Fe(II)<sub>total</sub> remaining (<math>\bar{X}</math>)</b>	10.54 ±2.77%	37.08 ±8.23%
<b>Fe(III) after NO<sub>2</sub><sup>-</sup> addition</b>	7.4%	9.9%
<b>Fe(III) after 28 days</b>	48.7%	*
<b>Mineral phase t<sub>ini</sub></b>	Vivianite	Vivianite
<b>Mineral phase t<sub>end</sub></b>	Vivianite/Ferrihydrite	*

256 \* Mössbauer sample ~~lost~~ *processing failed*

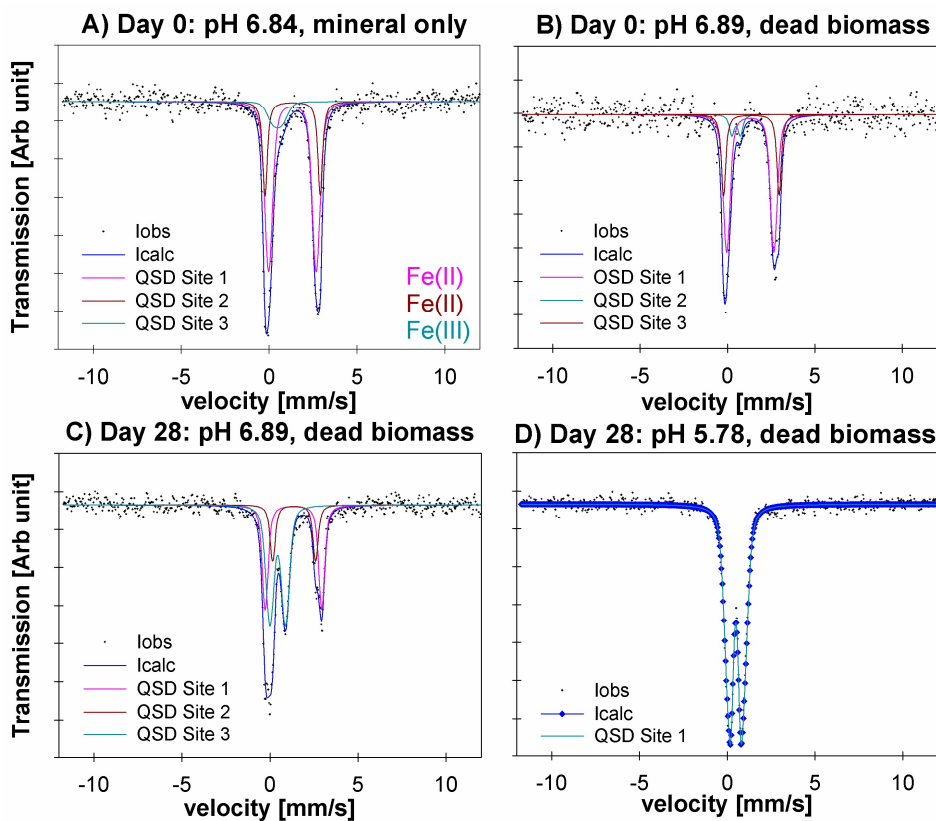
257

### 258 3.2. Fe mineral analysis

259 <sup>57</sup>Fe Mössbauer spectroscopy was used to quantify structural Fe(II) and Fe(III) contents of the samples and identify differences  
260 in mineralogy under the different reaction conditions. The hyperfine parameters of the mineral phases in in the mineral-only  
261 setup at t<sub>initial</sub> (pH 6.84) are dominated by Fe(II) doublets (Figure 3 A, QSD Sites 1 and 2), which most closely match that of a  
262 vivianite spectrum (Muehe et al., 2013; Veeramani et al., 2011). There is a small component with low centre shift and  
263 quadrupole splitting, indicative of Fe(III), which accounts for ~10% of the spectral area (Figure 3 A, QSD Site 3). This suggests  
264 some minor oxidation occurred, potentially during transfer of sample into the spectrometer. The mineral phases in the DB-  
265 amended setup at t<sub>initial</sub> (pH 6.89) shows very close approximation to the abiotic mineral-only setup, though with slightly less  
266 Fe(III) (~7.5% of the spectral area) (Figure 3 B, QSD Site 2). Precipitates analysed at the end of the DB-amended experiment  
267 (Day 28) show that at pH 6.89, the vivianite phase still dominates (Figure 3 C, QSD Sites 1 and 2), however, the Fe(III)  
268 component is now much more prominent (Figure 3 C, QSD Site 3), and suggests the formation of a poorly crystalline/short-  
269 ranged ordered mineral such as ferrihydrite (Cornell and Schwertmann, 2003). At the lowest pH (5.78) and in the presence of  
270 DB, the pattern of the precipitates is completely dominated by one doublet (Figure 3 C, QSD Site 1), with hyperfine parameters  
271 corresponding to a poorly ordered Fe(III) mineral such as ferrihydrite (Cornell and Schwertmann, 2003). Unfortunately, the  
272 *sample processing failed for the* mineral-only sample taken after 28 days *was lost* and can therefore not be used for further  
273 elucidations. Detailed fitting results of the <sup>57</sup>Fe Mössbauer spectroscopy are provided in Table 2.

274





275

276 Figure 3:  $^{57}\text{Fe}$  Mössbauer spectra collected at 77 K for (A) the mineral only setup precipitates at day 0 and pH 6.84, (B) the mineral  
 277 + dead biomass amended setup precipitates at day 0 at pH 6.89, (C) the mineral + dead biomass amended setup precipitates at day  
 278 28 and (D) the mineral + dead biomass amended setup precipitates at day 28 at pH 5.78. Full lines represent the calculated spectra  
 279 and their sums. Colours of the fits represent the corresponding Fe phase and thus vary between the graphs: Fe(II) doublets (A, C –  
 280 QSD Sites 1 and 2, B – QSD Sites 1 and 3) closely match the spectra known for vivianite. Minor amounts of Fe(III) are present at  
 281 day 0 in both, the mineral-only and DB-amended setups (A/B QSD Site 3/2). Single doublets shown in C (QSD Site 3) and D (QSD  
 282 Site 1) correspond to a poorly ordered Fe(III) mineral such as ferrihydrite.

283

284

285

286

287 **Table 2: Fitting results of Mössbauer spectroscopy. CS – centre shift, QS – quadrupole splitting, R.A. – Relative abundance**  
 288 **determined by integration under the curve, Chi<sup>2</sup> – goodness of fit; sample collection took place at t<sub>ini</sub> – initial time point and t<sub>end</sub> –**  
 289 **end time point; MO = mineral-only, MDB = mineral + dead biomass.**

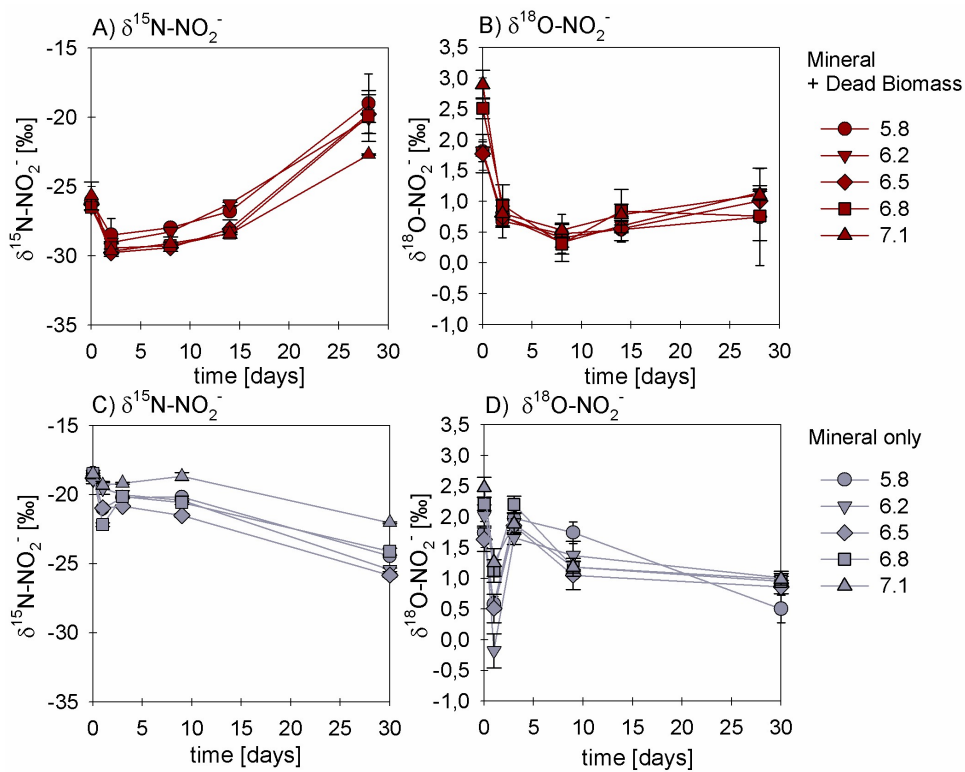
Sample	Temp [K]	Phase	CS [mm/s]	QS [mm/s]	R.A. [%]	Error	Chi <sup>2</sup>
MO_pH6.8_t <sub>ini</sub>	77	Fe(II)	1.32	2.71	66.0	23.0	0.55
		Fe(II)	1.33	3.15	24.0	23.0	
		Fe(III)	0.47	0.63	9.9	4.8	
MDB_pH6.8_t <sub>ini</sub>	77	Fe(II)	1.30	2.70	65.0	14.0	0.68
		Fe(III)	0.49	0.49	7.4	3.6	
		Fe(II)	1.36	3.18	28.0	15.0	
MDB_pH6.8_t <sub>end</sub>	77	Fe(II)	1.33	3.21	34.3	2.4	0.73
		Fe(II)	1.37	2.44	17.0	2.8	
		Fe(III)	0.44	0.89	48.7	2.4	
MDB_pH5.8_t <sub>end</sub>	77	Fe(III)	0.49	0.79	100.0		0.66

290

### 291 3.3. Nitrite and N<sub>2</sub>O isotope dynamics

292 In experiments with DB, the  $\delta^{15}\text{N-NO}_2^-$  and  $\delta^{18}\text{O-NO}_2^-$  values showed a very consistent initial  $\sim 3\text{--}4\%$ -decrease (from  $-26\%$   
 293 to  $-30\%$  for  $\delta^{15}\text{N}$  and from  $\sim +3\%$  to  $0\%$  for  $\delta^{18}\text{O}$ ) (Figure 4 A, B). After 5 days, the  $\delta^{15}\text{N}$  values started to increase again with  
 294 decreasing  $\text{NO}_2^-$  concentrations, reaching final values of  $\sim -20\%$  (Figure 4 A), whereas the concomitant increase in the  $\delta^{18}\text{O-}$   
 295  $\text{NO}_2^-$  was much smaller ( $<1\%$ , Figure 4 B). The same pattern was observed for all pH levels. In mineral-only experiments,  
 296 isotope trends were quite different. In combination with far less consumption of  $\text{NO}_2^-$ , the  $\delta^{15}\text{N-NO}_2^-$  values decreased  
 297 throughout the entire abiotic experiment (Figure 4 C). In contrast, the  $\delta^{18}\text{O-NO}_2^-$  first dropped by  $2\%$ , reaching a clear  
 298 minimum of  $\sim -0.5$  to  $-0.5\%$ , before rapidly increasing again. Over the remaining 25 days, the  $\delta^{18}\text{O-NO}_2^-$  slowly decreased  
 299 reaching final values of  $\sim 1\%$  (Figure 4 D) – similar to that of the [mineral plus](#) DB treatment.

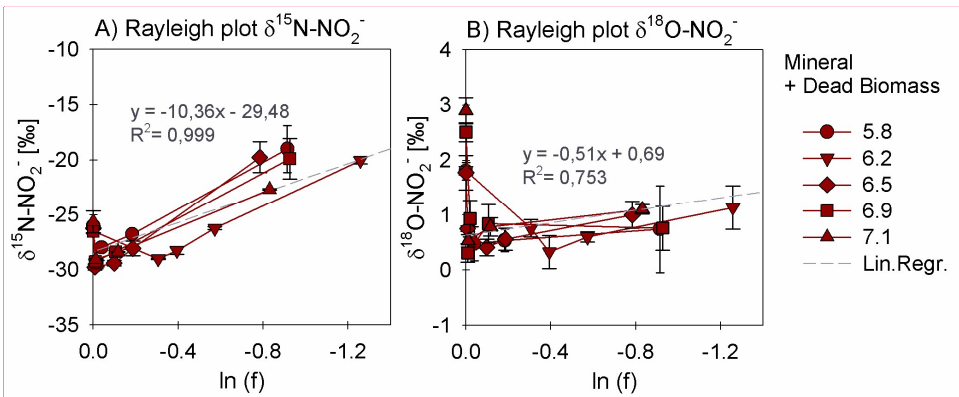
300



301  
 302 **Figure 4:**  $\delta^{15}\text{N}$  (A, C) and  $\delta^{18}\text{O}$  (B, D) values for  $\text{NO}_2^-$  measured in the mineral + dead biomass amended (red) and the mineral-only  
 303 (grey) setups over time and at different pH. Standard error calculated from biological replicates (n = 3) is represented by the error  
 304 bars.

305  
 306 In order to estimate the net N and O isotope fractionation for putative  $\text{NO}_2^-$  reduction (in the DB-amended experiments, where  
 307 we observed a clear decrease in  $\text{NO}_2^-$ ), we plotted the  $\text{NO}_2^-$   $\delta^{15}\text{N}$  and  $\delta^{18}\text{O}$  values against the natural logarithm of the  
 308 concentration of the residual  $\text{NO}_2^-$  (Rayleigh plot), where the slope of the regression line approximates the N and O isotope  
 309 effects, respectively (Mariotti et al., 1981). At least after the initial period, when the  $\text{NO}_2^-$   $\delta^{15}\text{N}$  markedly increased with  
 310 decreasing  $\text{NO}_2^-$  concentrations, the N isotope data are more or less consistent with Rayleigh isotope fractionation kinetics.  
 311 The slope of the regression line suggests an average N isotope effect of -10.4‰ (Figure 5 A). For the mineral-only setup, no  
 312 N isotope effect could be calculated, but the observed  $\text{NO}_2^-$   $\delta^{15}\text{N}$  trend suggest a small inverse N isotope fractionation (Figure

313 4 C). Similarly, trends in  $\text{NO}_2^-$   $\delta^{18}\text{O}$  of the DB experiments are not as obviously governed by normal Rayleigh fractionation  
 314 dynamics, at least not during the initial period, when the  $\delta^{18}\text{O}$  decreased despite decreasing  $\text{NO}_2^-$  concentrations. Considering  
 315 the  $\delta^{18}\text{O}$  values only after 2 days of the incubation, the Rayleigh plot revealed an average O isotope enrichment factor of -0.5  
 316 ‰ (Figure 5 B), much lower than for N. Similar to N, O-isotope Rayleigh plots for the mineral-only experiments (Figure S54)  
 317 did not exhibit coherent trends, as the fractional  $\text{NO}_2^-$  depletion was minor and not consistent (mostly less than 10%). Again,  
 318 the observed  $\delta^{18}\text{O}$  minimum at day 2 of the abiotic incubations suggests that processes other than normal kinetic fractionation  
 319 during  $\text{NO}_2^-$  reduction were at work, which cannot be described with the Rayleigh model. If at all, the decreasing  $\delta^{18}\text{O}$  values  
 320 after day 5 in the mineral-only experiments, accompanying the subtle decrease in  $\text{NO}_2^-$  concentration in at least some of the  
 321 treatments, suggest a small apparent inverse O isotope effect associated with the net consumption of  $\text{NO}_2^-$ . Despite the different  
 322  $\text{NO}_2^-$   $\delta^{18}\text{O}$  dynamics during the course of the experiment, the final  $\delta^{18}\text{O}$  of the residual nitrite was very similar in both  
 323 experimental setups, and independent of the pH.

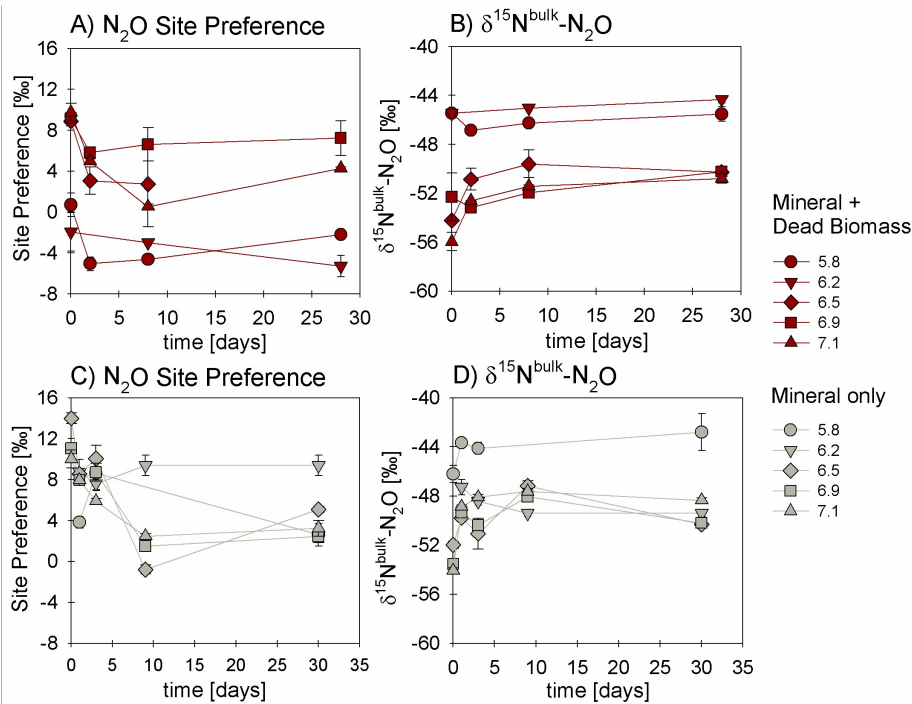


324  
 325 Figure 5: Rayleigh plots for  $\text{NO}_2^-$   $\delta^{15}\text{N}$  (A) and  $\delta^{18}\text{O}$  (B) values measured for the mineral + dead biomass amended setups over the  
 326  $\ln$  of the substrate fraction remaining and at different pH. The average linear regression line was calculated starting with the lowest  
 327 delta values (after the initial decrease in both  $\delta^{15}\text{N}$  and  $\delta^{18}\text{O}$  during the initial experimental phase). Equation and  $R^2$  are given in  
 328 grey. Standard error calculated from biological replicates ( $n = 3$ ) is represented by the error bars.

329  
 330 We also investigated the  $\text{N}_2\text{O}$  isotope dynamics during mineral-only and mineral plus DB DB-amended-incubations. Site  
 331 preference (SP) and  $\delta^{15}\text{N}^{\text{bulk}}$  of the  $\text{N}_2\text{O}$  produced in both experimental setups were plotted over time (Figure 5-6 A and B) and  
 332 show, except for a few values that require further investigation, almost no variation during the period of the experiment. Also,  
 333 disregarding the rather high and unusual (but well replicated) values already mentioned, the majority of values obtained in  
 334 both setups indicate that neither pH nor the amendment of DB seems to have had any influence on the isotopic composition of  
 335 the produced  $\text{N}_2\text{O}$  (Figure 5-6 B vs. D). Over the course of the experiment,  $\delta^{15}\text{N}^{\text{bulk}}$   $\text{N}_2\text{O}$  values were around  $-50 \pm 5\%$ . SP

Kommentiert [AV3]: Changed title x-axis to  $\ln(f)$

336 was relatively low, ranging roughly between -40 and a maximum of +140‰ (Figure 5-6 A, C), without any significant temporal  
 337 change.



338  
 339 **Figure 6: Site Preference (SP; A, C) and  $\delta^{15}\text{N}^{\text{bulk}}$  (B, D) values of  $\text{N}_2\text{O}$  produced in experiments amended with mineral + dead biomass**  
 340 **(red) and mineral-only (grey). For pH 6.5, the final SP value (A) is missing due to analytical problems (overly large sample peak**  
 341 **areas in the raw data) which biased the results. Standard error calculated from biological replicates (n = 3 or 23, extreme values N**  
 342 **= 2) is represented by the error bars.**

343  
 344 Rayleigh diagrams, in which  $\delta^{15}\text{N}^{\text{a}}$ ,  $\delta^{15}\text{N}^{\text{bulk}}$  and SP of the  $\text{N}_2\text{O}$  were plotted against concentrations of the reactant ( $\text{NO}_2^-$ )  
 345 remaining (Figure S6S5), confirm the similar  $\text{N}_2\text{O}$  isotope dynamics in the DB vs. mineral-only setups, despite the differential  
 346 degree of  $\text{NO}_2^-$  reduction (only minor in the mineral-only experiment, with f always greater 0.9) and despite the different  $\text{NO}_2^-$   
 347 N and O isotope dynamics. Similarly, the dual  $\text{N}_2\text{O}$   $\delta^{18}\text{O}$  vs.  $\delta^{15}\text{N}^{\text{bulk}}$  signatures (with the exception of two data points; Figure  
 348 S6S7) were almost equivalent in both setups, implying that, although modes of  $\text{NO}_2^-$  reduction clearly differ, a similar  
 349 mechanism of nitrite-reduction-associated  $\text{N}_2\text{O}$  production exists in both setups. The N and O isotopic results are summarized  
 350 in Table 3 (see discussion).

Kommentiert [AV4]: Corrected graph

#### 351 4. Discussion and implications

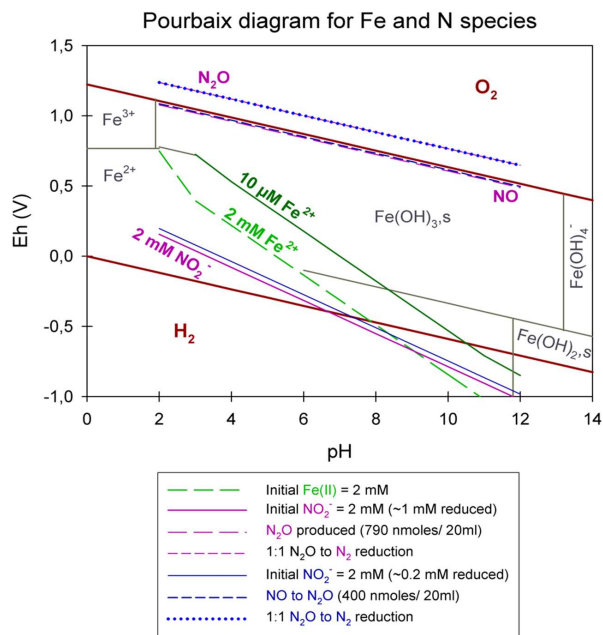
##### 352 4.1. General evaluation of the abiotic reaction systematics

353 Overall, the abiotic reaction between  $\text{NO}_2^-$  and Fe(II), heterogenous or homogenous, has been considered thermodynamically  
354 favourable, and as major contributor to the global  $\text{N}_2\text{O}$  budget (e.g. Jones et al., 2015; Otte et al., 2019). Previous studies on  
355 abiotic  $\text{NO}_2^-$  reduction with Fe(II) have usually been performed in the presence of rather high concentrations (>2 mM) of  $\text{NO}_2^-$   
356 and/or Fe(II), without taking into account that chemodenitrification is in fact considered to be highly concentration-dependent  
357 (Van Cleemput and Samater, 1995). In addition, reaction dynamics were often tested under variable conditions including the  
358 presence of different Fe(II)/Fe(III) minerals, sediments, organic materials and/or bacterial cells (Chen et al., 2018; Grabb et  
359 al., 2017; Otte et al., 2019). Whether  $\text{NO}_2^-$  indeed acts as a direct oxidant of Fe(II) at circumneutral pH or whether the reaction  
360 requires catalysis is still a matter of debate (Kampschreur et al., 2011; Sorensen and Thorling, 1991).

361 Integrating concentrations that are pertinent to our experiments, we constructed a Pourbaix diagram (e.g. Delahay et al., 1950;  
362 Minguzzi et al., 2012) (Figure 7). Based on these (simplified) thermodynamic calculations, the abiotic reaction solely driven  
363 by the reaction of  $\text{NO}_2^-$  and aqueous  $\text{Fe}^{2+}$  at a pH range of 5 to 7 is not supported. Under our experimental conditions,  $\text{Fe}^{2+}$  is  
364 predicted to be oxidized by NO rather than  $\text{NO}_2^-$ . Considering Figure 7, an accumulation of NO at  $\mu\text{M}$  or even mM  
365 concentrations would result in a downward shift of the  $\text{NO}_2^-$  line. Therefore, an accumulation of NO would only lower the  
366 reactivity between  $\text{NO}_2^-$  and  $\text{Fe}^{2+}$ , which implies that  $\text{NO}_2^-$  is not oxidizing  $\text{Fe}^{2+}$ . Again, this also implies that the reactivity  
367 between  $\text{NO}_2^-$  and  $\text{Fe}^{2+}$  is only enhanced if NO concentrations are rather low (pM range). In order to avoid NO accumulation  
368 and thus to enhance the abiotic reaction between  $\text{NO}_2^-$  and  $\text{Fe}^{2+}$ , NO would need to react further (either with  $\text{Fe}^{2+}$  or otherwise).  
369 This would induce a reaction cascade, resulting in the constant reduction of  $\text{NO}_2^-$  and NO, and thus in higher  $\text{N}_2\text{O}$   
370 concentrations. In contrast, if NO does accumulate as previously reported, the reaction between  $\text{NO}_2^-$  and  $\text{Fe}^{2+}$  would be  
371 suppressed and only NO could be reduced further to  $\text{N}_2\text{O}$ , a reaction that of course also depends on gas equilibration dynamics  
372 occurring with the headspace of the system. Nevertheless, considering all these aspects, including the fact that the  $\text{N}_2\text{O}$   
373 produced corresponds only to a minor fraction of the initial  $\text{NO}_2^-$  reduced, NO acting as main oxidizing agent seems more  
374 likely. The reaction mechanisms in this system are, however, complex and we note that this simplified thermodynamic analysis  
375 does neglect catalytic effects that are possibly induced by reactive surfaces. The complexity of this system is further indicated  
376 by the fact that, according to the Pourbaix diagram, a pH response towards  $\text{N}_2\text{O}$  accumulation would be expected which has,  
377 however, never been reported so far. Furthermore, testing various pH did not reveal an obvious pH effect on the reaction  
378 dynamics. Changes in pH will most certainly affect interactions between species such as HNO,  $\text{NO}_2$  and  $\text{N}_2\text{O}$  and thus could  
379 impact the reaction dynamics. **In addition, the results observed in the setup biased by accidentally adding twice as much  $\text{NO}_2^-$**   
380 **(DB, pH 5.8) do not differ from the results of the other setups and thus might question the previously mentioned concentration**  
381 **dependency (i.e.  $[\text{NO}_2^-]$ ).** It appears that, for a more detailed understanding of this redox system, the reactants/intermediates  
382 involved and thus the specific reaction kinetics would need to be determined. Unfortunately, quantification of these  
383 intermediates is hampered by their high reactivity, transient nature, and lack of detection techniques that can be applied in



384 batch culture experiments. Since low amounts (e.g., pM) of NO suffice to impact reaction dynamics and thus stimulate the  
 385 reaction between  $\text{NO}_2^-$  and  $\text{Fe}^{2+}$ , NO quantification could be crucial to assess the environmental controls on Fe(II)-coupled  
 386 chemodenitrification. In laboratory biological denitrification experiments, accumulation of NO has been reported (Goretski  
 387 and Hollocher, 1988; Zumft, 1997) and was shown to even account for up to 40% of the initial  $\text{NO}_3^-$  amended (Baumgärtner  
 388 and Conrad, 1992; Choi et al., 2006; Kampschreur et al., 2011; Ye et al., 1994; Zumft, 1997). Hence, Kampschreur et al.,  
 389 (2011) concluded that chemodenitrification is not necessarily solely caused by a single-step reaction, and proposed that the  
 390 oxidation of  $\text{Fe}^{2+}$  is rather caused by a two-step mechanism. They observed an immediate formation and accumulation of NO  
 391 after  $\text{NO}_2^-$  was added to  $\text{Fe}^{2+}$ , and as soon as a considerable fraction of the  $\text{Fe}^{2+}$  was oxidized,  $\text{N}_2\text{O}$  formation was detected.  
 392 Although NO and other possible intermediate (e.g.  $\text{NO}_2(\text{g})$ ) concentrations might not play a major role with regard to mass  
 393 balance considerations, their possible impact on the overall reaction systematics as well as the isotopic fractionation, remains  
 394 unclear.



395  
 396 **Figure 7:** Pourbaix diagram depicting an Fe and N-species based system. Overall calculations are based on the Nernst equation using  
 397 values taken from literature (for equation and values see table S1). **Green lines** represent  $\text{Fe}^{2+}$  concentrations, **pink lines** represent  
 398  $\text{NO}_2^-$  reduction experiments, starting with 2 mM  $\text{NO}_2^-$ , resulting in the reduction of 1 mM  $\text{NO}_2^-$ , the production of 790 nmol /20 ml  
 399  $\text{N}_2\text{O}$  and a 1:1 transformation of  $\text{N}_2\text{O}$  to  $\text{N}_2$ ; **blue lines** represent  $\text{NO}_2^-$  reduction experiments, starting with 2 mM  $\text{NO}_2^-$ , resulting in  
 400 the reduction of 0.2 mM  $\text{NO}_2^-$ , the production of 790 nmol /20 ml  $\text{N}_2\text{O}$  and a 1:1 transformation of  $\text{N}_2\text{O}$  to  $\text{N}_2$ . Reduction/production  
 401 values were taken from our results presented in 3.1.

#### 402 4.2. Surface catalysis of chemodenitrification

403 Previous studies have shown that the initial presence of either Fe(III)(oxyhydr)oxides (Coby & Picardal, 2005; Klueglein &  
404 Kappler, 2013; Sorensen & Thorling, 1991) or amorphous Fe(II) minerals (Van Cleemput and Samater, 1995) can stimulate  
405 the abiotic reaction between  $\text{NO}_2^-$  and  $\text{Fe}^{2+}$ . As summarized in Table 1, under mineral-only conditions  $\text{NO}_2^-$  reduction was  
406 significantly lower ( $0.004 \pm 0.003 \text{ mmol L}^{-1} \text{ day}^{-1}$ ) than in identical experiments containing DB, which substantially enhanced  
407  $\text{NO}_2^-$  reduction ( $0.053 \pm 0.013 \text{ mmol L}^{-1} \text{ day}^{-1}$ ). The catalytic effect of Fe minerals on the abiotic  $\text{NO}_2^-$  reduction, which has  
408 been demonstrated before, seems to be amplified in the presence of DB. Relative to  $\text{NO}_2^-$  reduction rates, overall final  $\text{N}_2\text{O}$   
409 yields per mole  $\text{NO}_2^-$  reduced tended to be higher in the mineral-only setups. However, considering the initial  $\text{NO}_2^-$   
410 concentrations, only minor amounts of  $\text{N}_2\text{O}$  were produced in both setups, raising questions about the contribution of  
411 chemodenitrification to global  $\text{N}_2\text{O}$  emissions discussed by others (Grabb et al., 2017; Jones et al., 2015; Otte et al., 2019;  
412 Zhu-Barker et al., 2015). For example, in comparison to the  $\text{N}_2\text{O}$  yields in experiments where chemodenitrification was  
413 catalysed by green rust (up to 31%, Grabb et al., 2017), the amount of  $\text{N}_2\text{O}$  produced in our setups is far lower (<5% of the  
414 initial  $\text{NO}_2^-$ ).

415 Fe-bearing minerals are known for their high reactivity, ability to complex ligands (metals, humics) and phosphates, and  
416 surface protonation capacity via the sorption of OH<sup>-</sup> groups (Elsner et al., 2004; Stumm and Sulzberger, 1992). Surface  
417 catalytic effects may include *direct* and *indirect* sorption-induced catalysis. In the environment, pH has been shown to have a  
418 strong influence on these sorption capacities of Fe minerals in general (Fowle and Konhauser, 2011). Considering the point of  
419 zero charge (PZC) of vivianite, which is with 3.3 below the lowest tested pH in our experiments, the mineral surface is  
420 positively charged under our experimental conditions (Luna-Zaragoza et al., 2009). Hence the pH range tested here will not  
421 affect the surface charge, and  $\text{NO}_2^-$  sorption onto mineral surfaces and corresponding heterogeneous reactions are possible. In  
422 contrast, cell surfaces are considered to be negatively charged (Wilson et al., 2001) and therefore might induce different effects  
423 than mineral surfaces. The charge of the cell surface most likely remained negative even after autoclaving (see e.g. Halder et  
424 al., 2015). Our results imply that the systematics of chemodenitrification are strongly dependent on the surface provided and  
425 that, depending on the availability and quality of catalytic surfaces, Fe coupled chemodenitrification may be a single-step  
426 reaction (between  $\text{NO}_2^-$  and Fe) or may occur in multiple steps (reaction between Fe and  $\text{NO}_2^-$ , as well as Fe and NO). As a  
427 consequence, the nature of surface catalysis would likely have a strong impact on the  $\text{N}_2\text{O}$  yield per mole  $\text{NO}_2^-$  reduced to NO.  
428 Since NO has been demonstrated to have a ~~strong rather exceptional~~ affinity towards  $\text{Fe}^{2+}$  and  $\text{Fe}^{3+}$  centres resulting in the  
429 formation of  $\text{Fe}^{\text{x+}}(\text{NO})_n$  nitrosyls and thus triggering an enhancement of the  $\text{N}_2\text{O}$  decomposition rate (e.g. Rivallan et al., 2009).  
430 It remains unclear to what extent, and why, the quality of the catalytic surfaces plays a role. Particularly in the presence of  
431 organics and/or dead bacterial cells, which are known to have a high affinity to bind metal ions (e.g.  $\text{Ni}^{2+}$ ,  $\text{Cu}^{2+}$  or  $\text{Zn}^{2+}$ ), either  
432 directly or by forming surface complexes with hydroxyl groups (Fowle and Konhauser, 2011), a surface-catalysis-induced  
433 reaction can be expected. Besides acting as a catalyst via a reactive surface, the dead biomass might also have directly triggered  
434 the reaction. For example, non-enzymatic NO formation was studied and modelled by Zweier et al. (1999), suggesting that at

435 concentrations between 100 and 1000  $\mu\text{M}$ , abiotic  $\text{NO}_2^-$  disproportionation and thus NO formation at circumneutral pH in  
436 organic tissue is still possible (Zweier et al., 1999). Furthermore, autoclaving might have ruptured cell walls and released  
437 organic compounds. In the presence of phenolic compounds, humic substances, and other organic compounds,  $\text{NO}_2^-$  has been  
438 shown to form NO via self-decomposition (Nelson and Bremner, 1969; Stevenson et al., 1970; Tiso and Schechter, 2015).  
439 Whether this may have been the case also in our experiments remains unclear, since we did not conduct experiments containing  
440 only DB and  $\text{NO}_2^-$ . Another possible consideration is the presence of extracellular polymeric substances (EPS), which should  
441 also be tested in future studies. Liu et al., (2018) investigated nitrate-dependent Fe(II) oxidation with *Acidovorax* sp. strain  
442 BoFeN1, showing that *c*-cytochromes were present in EPS secreted which could indeed act as electron shuttling agents  
443 involved in electron transfer supporting chemolithotrophic growth. Since *S. oneidensis*, our model organisms used as DB  
444 supply, is known to produce large amounts of EPS, harbouring *c*-cytochromes (Dai et al., 2016; Liu et al., 2012; White et al.,  
445 2016), a potential impact of EPS on the reaction between  $\text{NO}_2^-$  and Fe(II) needs to be considered. However, possible  
446 cytochromes present in the EPS most likely lost their activity due to protein denaturation during autoclaving (Liu &  
447 Konermann, 2009; Tanford, 1970). Nevertheless, EPS is still present and can act as a catalysing agent to the abiotic reaction  
448 mechanism (Klueglein et al., 2014; Nordhoff et al., 2017).  
449 Fe(II)<sub>total</sub> oxidation via  $\text{NO}_2^-$  has also been observed in the mineral-only setups, but to a lower extent. Hence, the vivianite  
450 mineral surfaces themselves seem to catalyse the abiotic reaction between  $\text{NO}_2^-$  and Fe(II)/  $\text{Fe}^{2+}$  (in parts, the stimulation of  
451 Fe-dependent nitrite reduction may also be attributed vivianite dissolution providing ample Fe(II) substrate). Previous studies  
452 reported on mineral-enhanced chemodenitrification (Dhakal et al., 2013; Grabb et al., 2017; Klueglein & Kappler, 2013;  
453 Rakshit et al., 2008), and the catalytic effect may be due to  $\text{NO}_2^-$  adsorption onto the minerals surface possibly facilitating a  
454 direct electron transfer. Similar findings have been reported previously on Fe(II) oxidation promoted by electron transfer  
455 during adsorption onto a Fe(III) minerals surface (Gorski and Scherer, 2011; Piasecki et al., 2019).  $\text{OH}^-$  adsorption is probably  
456 enabled by the minerals positive surface charge at pH >6, resulting in a limited reactive surface availability. Complexation of  
457 dissolved  $\text{Fe}^{2+}$ , which is provided by mineral dissolution, by  $\text{OH}^-$  groups would thus result in a lower overall  $\text{NO}_2^-$  reduction  
458 rate compared to the DB-amended setups. Nevertheless, the NO formed by the initial  $\text{NO}_2^-$  reduction could, at still elevated  
459  $\text{Fe}^{2+}$  levels, proceed until both dissolved and adsorbed Fe(II) is quantitatively oxidized to surface-bound Fe(III) (Kampschreur  
460 et al., 2011). This would ultimately lead to similar Fe(II)<sub>total</sub> oxidation and  $\text{N}_2\text{O}$  production (and thus higher  $\text{N}_2\text{O}$  yields) as in  
461 the DB amended experiment and thus explain the similar results.

#### 462 4.3. Mineral alteration during Fe-coupled chemodenitrification

463 We used  $^{57}\text{Fe}$  Mössbauer spectroscopy in order to determine, whether the catalytic effects that enhanced chemodenitrification  
464 with  $\text{Fe}^{2+}$  also modulated mineral formation. In both setups, addition of  $\text{Fe(II)Cl}_2$  to the 22 mM bicarbonate buffered medium  
465 led to the formation of vivianite, an Fe(II)-phosphate. Shortly after the addition of  $\text{Fe}^{2+}_{\text{aq}}$ , the mineral phase in both setups was  
466 dominated by Fe(II), but a small fraction of Fe(III) was also present. Initial fractions of Fe(III) were similar in both the mineral-  
467 only and DB-amended experiments (9.9% and 7.4%, respectively) and, if not an artefact of Mössbauer sample handling, might

468 therefore have stimulated Fe(II) adsorption and oxidation (Gorski and Scherer, 2011; Piasecki et al., 2019). The reduction of  
469  $\text{NO}_2^-$  was accompanied by a marked increase of Fe(III), likely in the form of short-range ordered ferrihydrite or lepidocrocite.  
470 Thus, the Fe(III) phase detected at day 0 most likely formed immediately after  $\text{NO}_2^-$  addition. This is supported by prior studies,  
471 which demonstrated the initiation of Fe(II) oxidation with  $\text{NO}_2^-$  within a short period of time (Jamieson et al., 2018; Jones et  
472 al., 2015). At the end of the DB experiment at pH 6.89, oxidized Fe(III) (most likely in the form of poorly ordered ferrihydrite)  
473 contributed 48.7% to the total Fe phases, with vivianite accounting for the remaining spectral area. Unfortunately, we are  
474 unable to compare the results of the DB-amended precipitates at the end of the experiment to the mineral-only setup, since the  
475 sample was lost/processing failed. In contrast to our observations, other studies conducted in the presence of organics have  
476 identified goethite as the main Fe(III) phase during the abiotic reaction between Fe(II) and  $\text{NO}_2^-$  (Chen et al., 2018; Liu et al.,  
477 2018). In NDFeO experiments, the formation of lepidocrocite, goethite, hematite and to some extent, magnetite has been  
478 reported. Minerals obtained from the enrichment culture KS were mostly vivianite and ferrihydrite, which is, however,  
479 attributed to the fact that for the cultivation of the KS culture a high-phosphate medium is used (Nordhoff et al., 2017). In the  
480 abiotic experiments (10 mM Fe(II) and 10 mM  $\text{NO}_2^-$ ) presented by Jones et al., (2015), the formation of lepidocrocite, goethite  
481 and two-line ferrihydrite were observed after 6 to 48 hrs. In the experiments presented here, besides a short-range ordered  
482 Fe(III) phase, likely ferrihydrite, no other mineral phases could be identified after 28 days.

483 Iron analysis also indicates that the oxidation of the  $\text{Fe(II)}_{\text{total}}$  went to completion at pH 5.8 whereas at pH 6.8, 52.3% of the  
484  $\text{Fe(II)}_{\text{total}}$  remained at the end of the incubation experiment, resulting in the formation of a poorly-ordered ferrihydrite.  
485 Unfortunately, we did not measure the zeta potential of the starting solutions, which would probably help to explain the  
486 differences detected. We note that, although  $^{57}\text{Fe}$  Mössbauer spectroscopy was used to measure the Fe(II)/Fe(III) in the  
487 precipitates, the reported  $\text{Fe(II)}_{\text{total}}$  concentrations reflect the total Fe(II), i.e., of both the dissolved pellet (structurally-bound  
488 or adsorbed) and the aqueous  $\text{Fe}^{2+}$  in the supernatant measured by Ferrozine. The results obtained by Mössbauer analysis (50%  
489 Fe(II) remaining) seem to contradict the ferrozine assay (<10% remaining) (see Table 1 and 2). The presence of ferrous Fe,  
490 either as structurally-bound Fe(II) or adsorbed  $\text{Fe}^{2+}$  does indeed play a crucial role with regards to the reaction dynamics  
491 occurring at the mineral surfaces, particularly if we assume that N-reactive species are also still present (Rivallan et al., 2009).  
492 In addition, the initially formed Fe(III) phase might also induce another feedback to the N and even the Fe cycle since Fe(III)  
493 minerals are also highly reactive (Grabbe et al., 2017; Jones et al., 2015). Mineral structure and thus Fe(II) location within the  
494 lattice can influence the overall Fe accessibility, the binding site at the mineral surface and thus overall reactivity (Cornell and  
495 Schwertmann, 2003; Luan et al., 2015; Schaefer, 2010). If the initial formation of Fe(III), however, enhanced the reaction  
496 between  $\text{NO}_2^-$  and Fe(II), similar results in both setups should have been observed, which this was not the case since  $\text{NO}_2^-$   
497 reduction patterns in the mineral-only experiments were much lower. This also indicates again, that the presence of DB indeed  
498 contributed greatly to the reaction in the DB experiments. Furthermore, results obtained from Mössbauer analysis are the only  
499 results supporting a pH-dependent effect: At pH 5.78 and in the presence of DB, all vivianite was fully transformed into a  
500 short-range ordered Fe(III) phase whereas at pH 6.89, vivianite remained a major component. This presence of vivianite also  
501 indicates that no further Fe(II) oxidation occurred even though  $\text{NO}_2^-$  reduction was incomplete. The incomplete reduction of

502 NO<sub>2</sub><sup>-</sup> in turn suggests that further Fe(II) oxidation was limited due to blocked or deactivated reaction sites on mineral surfaces.  
503 Also, considering that at pH 5.8 and in the presence of DB, the initial NO<sub>2</sub><sup>-</sup> concentrations were higher but the overall reaction  
504 dynamics were quite similar to the other reaction conditions, the concentration dependency of the reaction between NO<sub>2</sub><sup>-</sup> and  
505 Fe(II) is again supported.

#### 506 4.4. Nitrite and N<sub>2</sub>O N and O isotope dynamics during chemodenitrification

507 In the presence of only vivianite, a decrease in δ<sup>15</sup>N-NO<sub>2</sub><sup>-</sup> of ~3‰ ~~was observed with the initial decrease occurred in parallel~~  
508 ~~with initially decreasing in~~ NO<sub>2</sub><sup>-</sup> concentrations. Initial δ<sup>18</sup>O-NO<sub>2</sub><sup>-</sup> values also reflect this drop of 3‰ during the first 3 days  
509 but level off and stabilize at 1‰ after 9 days. The initial decrease in both δ<sup>15</sup>N and δ<sup>18</sup>O of NO<sub>2</sub><sup>-</sup> suggest apparent inverse  
510 isotope effects, which to the best of our knowledge have never been observed during chemodenitrification, and have only been  
511 reported for enzymatic NO<sub>2</sub><sup>-</sup> oxidation (Casciotti, 2009). Since biological NO<sub>2</sub><sup>-</sup> oxidation can be ruled out (no NO<sub>3</sub><sup>-</sup> produced,  
512 no microbes), the decrease in δ<sup>15</sup>N-NO<sub>2</sub><sup>-</sup>, though subtle, could indicate that either heavy isotopes are incorporated in the  
513 products formed (i.e. NO, N<sub>2</sub>O), at least at the beginning of the incubation period. Normally, the heavier isotopes build  
514 compounds with molecules of higher stability (Elsner, 2010; Fry, 2006; Ostrom & Ostrom, 2011). This is particularly true for  
515 the formation of some minerals or highly stable molecules that are formed under mineral-only conditions, where processes can  
516 reach an isotopic equilibrium (He et al., 2016; Hunkeler & Elsner, 2009; Li et al., 2011; Ostrom & Ostrom, 2011). However,  
517 in the system presented here, N incorporation into mineral phases can be excluded, hence another process must favour the  
518 heavy N-atoms. Since this initial drop in δ<sup>15</sup>N was also observed in the DB-amended experiments, a possible explanation might  
519 be that the isotope values here reflect the sorption or complexation mechanism of NO<sub>2</sub><sup>-</sup> onto the reactive surfaces. In contrast  
520 δ<sup>18</sup>O-NO<sub>2</sub><sup>-</sup> values, after the initial decrease, did not change greatly with decreasing NO<sub>2</sub><sup>-</sup> concentrations. The stabilization of  
521 the δ<sup>18</sup>O-NO<sub>2</sub><sup>-</sup> towards the end of the experiment most likely reflects the oxygen isotope equilibration between δ<sup>18</sup>O-NO<sub>2</sub><sup>-</sup> and  
522 the δ<sup>18</sup>O of the water in the medium. Temporal δ<sup>18</sup>O-NO<sub>2</sub><sup>-</sup> dynamics did not change greatly between the different pH treatments,  
523 and in all cases the final δ<sup>18</sup>O-NO<sub>2</sub><sup>-</sup> ranged between 0.5 and 1‰. The kinetics of abiotic O-atom exchange is a function of  
524 temperature and pH. At near neutral pH, at room temperature, one can expect NO<sub>2</sub><sup>-</sup> to be fully equilibrated after two to three  
525 days (Casciotti et al., 2007). At higher pH, the first order rate constants for the equilibration with water are lower (Buchwald  
526 and Casciotti, 2013), but equilibrium conditions should have been reached well within the incubation period. Indeed, the final  
527 δ<sup>18</sup>O-NO<sub>2</sub><sup>-</sup> was consistent with an equilibrium O isotope effect between NO<sub>2</sub><sup>-</sup> and H<sub>2</sub>O with a δ<sup>18</sup>O of ~-11.5‰ (Buchwald and  
528 Casciotti, 2013). With regards to δ<sup>15</sup>N-NO<sub>2</sub><sup>-</sup> values of the DB-amended experiments, a similar behaviour is found within the  
529 first 3 days (i.e., decrease in δ<sup>15</sup>N), followed by a clear increase in δ<sup>15</sup>N-NO<sub>2</sub><sup>-</sup> of ~10‰. While it is difficult to explain the  
530 initial decrease in δ<sup>15</sup>N-NO<sub>2</sub><sup>-</sup> (a feature that was not observed in other chemodenitrification experiments (i.e. Grabb et al., 2017;  
531 Jones et al., 2015), the subsequent increase in δ<sup>15</sup>N can be attributed to normal isotopic fractionation associated with  
532 chemodenitrification and an N isotope effect (-9‰) that is consistent with those previously reported on Rayleigh-type N and  
533 O isotope kinetics during chemodenitrification with Fe(III)-bearing minerals such as nontronite and green rust (Grabb et al.,  
534 2017). In contrast, δ<sup>18</sup>O-NO<sub>2</sub><sup>-</sup> values initially decrease as in the abiotic experiment but then level off faster reaching final values

535 of ~1‰, again most likely explained by O atom isotope exchange pulling the  $\delta^{18}\text{O}\text{-NO}_2^-$  values towards the O-isotope  
536 equilibrium value. This value is given by the  $\delta^{18}\text{O}_{\text{H}_2\text{O}} + {}^{18}\epsilon_{\text{eq,NO}_2^-}$ , whereas the latter is defined as the equilibrium isotope effect  
537 between  $\text{NO}_2^-$  and  $\text{H}_2\text{O}$  and has been shown to yield values of roughly +13‰ (Casciotti et al., 2007). Overall, it seems that the  
538 non-linear behaviour of the  $\text{NO}_2^-$  in the O isotope Rayleigh plot is most likely due to the combined effects of kinetic O isotope  
539 fractionation during  $\text{NO}_2^-$  reduction, and O atom exchange between  $\text{NO}_2^-$  and  $\text{H}_2\text{O}$ .

540  $\text{NO}_2^-$  N and O isotope trends observed under the DB-amended conditions (in which a large portion of the  $\text{NO}_2^-$  pool was  
541 consumed), somewhat contradict prior reports of chemodenitrification exhibiting a clear increase in both  $\delta^{15}\text{N}$  and  $\delta^{18}\text{O}\text{-NO}_2^-$ ,  
542 with N isotope enrichment factors for  $\text{NO}_2^-$  reduction between -12.9 and -18.1‰ and an O isotope effect of -9.8‰ (Jones et  
543 al., 2015). Consistent with our data, however, they also observed that, at least in abiotic experiments where  $\text{NO}_2^-$  consumption  
544 is rather sluggish due to  $\text{Fe}^{2+}$  limitation (as a result of either oxidation or simply occlusion), O-isotope exchange isotope effects  
545 mask the effects of kinetic O isotope fractionation. While we cannot say at this point what exactly governs the combined  $\text{NO}_2^-$   
546 N vs. O isotope trends in the two different experimental conditions, we observed that the two processes (water isotope  
547 equilibrium and KIE) competing with each other lead to different net dual isotope effects. Our data cannot resolve whether  
548 these observations reflect fundamental differences or simply changes in the relative proportion of the competing processes.  
549 Nevertheless, our observations may still be diagnostic for chemodenitrification catalysed by a mineral surface on the one hand,  
550 and Fe-coupled chemodenitrification that involves catalytic effects by dead bacterial cells on the other. The mineral catalyst  
551 evidently plays an important role with regards to chemodenitrification kinetics, reaction conditions, surface complexation or  
552 contact time between the  $\text{NO}_2^-$  substrate and the mineral phase (Samarkin et al., 2010), and in turn the combined  
553 kinetic/equilibrium N and O isotope effects.

554 The  $\Delta^{15}\text{N}$  values ( $\Delta^{15}\text{N} = \delta^{15}\text{N}_{\text{nitrite}} - \delta^{15}\text{N}_{\text{N}_2\text{O}^{\text{bulk}}}$ ) presented in Table 3 were obtained by subtracting the average  $\delta^{15}\text{N}^{\text{bulk}}$  value of  
555  $\text{N}_2\text{O}$  (abiotic  $-496.5 \pm 0.26\text{‰}$ ; dead biomass  $-50.549.4 \pm 1.0.8\text{‰}$ ) across all pH and throughout the experiment from the average  
556 of the initial  $\delta^{15}\text{N}_{\text{nitrite}}$  value. These values can provide insight on reaction kinetics between  $\text{NO}_2^-$ ,  $\text{NO}$ , and  $\text{N}_2\text{O}$  (Jones et al.,  
557 2015). In both setups there is an offset between the  $\text{NO}_2^-$  and  $\text{N}_2\text{O}$   $\delta^{15}\text{N}$ , which is clearly higher than what would be expected  
558 based on the  $\text{NO}_2^-$  reduction  $\text{NO}_2^-$  isotope effect of <10‰. Following the argumentation of Jones et al. (2015), who reported a  
559 similar N isotopic offset between  $\text{NO}_2^-$  and  $\text{N}_2\text{O}$  of  $27.0 \pm 4.5\text{‰}$ , this could be indicative for a heavy N accumulating in a  
560 forming  $\text{NO}$  pool, whereas  $^{14}\text{N}$  is preferentially reacting to  $\text{N}_2\text{O}$  or  $\text{N}_2$ , respectively. This might even be supported by the rather  
561 low  $\delta^{15}\text{N}^{\text{bulk}}$  values detected for  $\text{N}_2\text{O}$  in both setups.

562  
563  
564  
565  
566

567 **Table 3: Comparison of the isotope values obtained during dead biomass versus the abiotic experiments. T0 values represent means**  
568 **calculated by summarizing results across all pH  $\pm$  standard error.  $\delta^{15}\text{N}$  and  $\delta^{18}\text{O}$  values were calculated using  $\bar{x}_{t_0} - \bar{x}_{t_{end}}$ , whereas**

**Kommentiert [ML5]:** Make sure the table is not split over two different pages

569 **an overall increase from the initial value is marked with ↑, and a decrease with ↓. The calculated isotope fractionation factor (ε)**  
 570 **was calculated** is based on the slope between the lowest initial value (here at t<sub>i</sub>) and t<sub>end</sub> for all pH. Δ<sup>15</sup>N (= δ<sup>15</sup>N<sub>nitrite</sub> - δ<sup>15</sup>N<sub>2O<sup>bulk</sup></sub>) was  
 571 calculated for the end of the experiment.

	Dead Biomass	Abiotic
δ <sup>15</sup> N <sub>nitrite(t<sub>0</sub>-t<sub>end</sub>)</sub>	↑5.99 ±0.65‰	↓5.93 ±0.73‰
δ <sup>18</sup> O <sub>nitrite(t<sub>0</sub>-t<sub>end</sub>)</sub>	↓1.75 ±0.23‰	↓1.15 ±0.18‰
<sup>15</sup> ε <sub>nitrite</sub>	-10.36 ‰ <sup>#</sup>	-
<sup>18</sup> ε <sub>nitrite</sub>	-0.51‰ <sup>#</sup>	-
SP	<del>2.31</del> ↑1.7 ±1.2‰	<del>6.55</del> ↓9.99 ±0.84‰
δ <sup>15</sup> N <sup>a</sup>	<del>-48.95</del> ↑1.84 ±0.1‰	<del>-46.34</del> ↓3.53 ±0.046‰
δ <sup>15</sup> N <sub>bulk</sub>	<del>-49.38</del> 50.5 ±1.04 0.8‰	<del>-46.48</del> 49.5 ±2.10.6‰
Δ <sup>15</sup> N	<del>24.42</del> 3.2‰	<del>30.92</del> 7.85‰

572 <sup>#</sup> n=4 (t<sub>1</sub> to t<sub>end</sub>); - concentrations in abiotic experiment fluctuate and show only minor decrease, hence <sup>15</sup>ε and <sup>18</sup>ε could not be calculated.  
 573

574 While our results clearly showed that N<sub>2</sub>O accumulates over the course of the reaction, it remains unclear, which additional  
 575 end products are present at the final stage of the experiment. If NO accumulates (instead of following the reaction cascade  
 576 further), the substrate-product relationship between the δ<sup>15</sup>N-NO<sub>2</sub><sup>-</sup> and δ<sup>15</sup>N-N<sub>2</sub>O values that would be expected in a closed  
 577 system is perturbed, leading to significantly higher Δ<sup>15</sup>N than predicted by the δ<sup>15</sup>N-NO<sub>2</sub><sup>-</sup> trend. Hence, the calculated Δ<sup>15</sup>N of  
 578 the mineral-only treatment (30.927.9‰) is **only** slightly higher than that of the DB experiment (24.423.2‰), and would  
 579 therefore suggest that despite the differences in chemodenitrification kinetics (i.e., different NO<sub>2</sub><sup>-</sup> reduction rates and extent),  
 580 the NO pool formed is enriched in heavy N in both treatments, respectively. Alternatively, fractional reduction of the produced  
 581 N<sub>2</sub>O to N<sub>2</sub> may also affect the Δ<sup>15</sup>N since it would presumably increase the δ<sup>15</sup>N-N<sub>2</sub>O and thereby raise the low δ<sup>15</sup>N-N<sub>2</sub>O  
 582 closer to the starting δ<sup>15</sup>N-NO<sub>2</sub><sup>-</sup>. Abiotic decomposition of N<sub>2</sub>O to N<sub>2</sub> in the presence of Fe-bearing zeolites has been  
 583 investigated previously (Rivallan et al., 2009), however, it remains unclear if this process could also occur here. Fractional  
 584 N<sub>2</sub>O reduction is also not explicitly indicated by the SP values, which would reflect an increase with N<sub>2</sub>O reduction (Ostrom  
 585 et al., 2007; Winther et al., 2018). The SP values in both mineral-only and DB-amended experiments were, with some  
 586 exceptions, relatively low (6.50 ± 0.8‰; ~~2.31~~↑1.7 ± 1.2‰; Fig. 6, Table 3). In fact, SP values observed during the course of our  
 587 experiments are significantly lower compared to SP values reported in other studies on Fe-oxide-mineral associated  
 588 chemodenitrification (e.g., ~16‰; Jones et al. (2015); 26.5‰; Grabb et al. 2017), or during the abiotic N<sub>2</sub>O production during  
 589 the reaction of Fe and a NH<sub>2</sub>OH/NO<sub>2</sub><sup>-</sup> mixture (34‰; Heil et al. 2014). While the variety of different SP values for  
 590 chemodenitrification-derived N<sub>2</sub>O suggests different reaction conditions and catalytic effects, our SP data seem to imply that  
 591 the mineral catalyst plays only a minor role with regards to the isotopic composition of the N<sub>2</sub>O produced. However, since  
 592 N<sub>2</sub>O concentrations, even if minor, are increasing towards the end of the experiments, production and possible decomposition  
 593 as well as ongoing sorption mechanisms might also serve as possible explanation leading to these rather low SP values. N<sub>2</sub>O

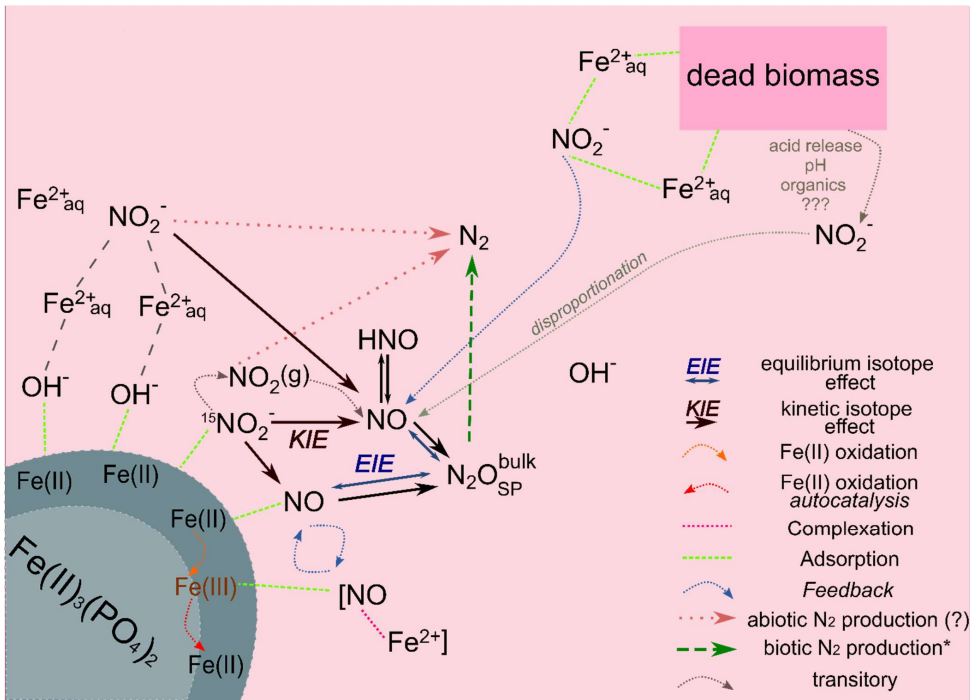
594 SP values have been used as valuable tracer for microbial N<sub>2</sub>O production (Ostrom & Ostrom, 2012). Based on pure culture  
595 studies (Ostrom et al., 2007; Winther et al., 2018; Wunderlin et al., 2013) and investigations in natural environments (Wenk  
596 et al., 2016) a SP range of -10 to 0‰ is considered to be characteristic for denitrification or nitrifier denitrification (Sutka et  
597 al., 2006; Toyoda et al., 2005), whereas higher values are usually attributed to nitrification or fungal denitrification (Ostrom  
598 & Ostrom, 2012; Wankel et al., 2017; Well & Flessa, 2009). The SP values reported here (0 to 140‰) fall well within the  
599 range of biological N<sub>2</sub>O production, explicitly denitrification and soil derived denitrification (2.3 to 16‰) (Ostrom & Ostrom,  
600 2012), rendering the separation between chemodenitrification and microbial denitrification based on N<sub>2</sub>O isotope  
601 measurements difficult, if not impossible.

602 In summary, the N and O isotope systematics of chemodenitrification are multifaceted, depending on the environmental  
603 conditions, reaction partners provided, and/or the speciation of precipitated mineral phases. The systematics observed here are  
604 clearly not entirely governed by normal kinetic isotope fractionation only, as has also been observed in previous work. Grabb  
605 et al. (2017) demonstrated that there is a relationship between reaction rate and kinetic NO<sub>2</sub><sup>-</sup> N and O isotope effects, with  
606 faster reaction leading to lower <sup>15</sup>ε and <sup>18</sup>ε. Again, changes in the expression and even in the direction of the isotope effects in  
607 the NO<sub>2</sub><sup>-</sup> pool suggest that multiple processes, including equilibrium isotope exchange (at least with regards to the δ<sup>18</sup>O- NO<sub>2</sub><sup>-</sup>  
608 ), are contributing to the net N and O isotope fractionation regulated by the experimental conditions and reaction rates. As  
609 pointed out by Grabb et al. (2017), and as supported by our comparative study with pure abiotic mineral phases and with added  
610 dead biomass, the accessibility of Fe(II) to the reaction may be a key factor regarding the degree of N and O isotope  
611 fractionation expressed, particularly if complexation limits the reactive sites of the mineral. The conditions that, at least  
612 transiently, lead to the apparent inverse N and O isotope fractionation observed here for chemodenitrification requires  
613 particular attention by future work. At this point, we can only speculate about potential mechanisms, which are indicated in  
614 the conceptual illustration (Figure 8). As chemodenitrification seems to be catalysed by reactive surfaces of Fe(II)/Fe(III)-  
615 minerals and/or organics (including cells), sorption onto these surfaces might play a crucial role in the fractionation of N and  
616 O isotopes. For example, during the catalytic hydrogenation of CO<sub>2</sub> on Fe and Co catalysts, a subtle depletion (ca. 4‰) in  
617 <sup>13</sup>CO<sub>2</sub> at progressed conversion to methane has been explained by the precipitation of a <sup>13</sup>C-enriched carbon intermediate (e.g.,  
618 CO-graphite) on the catalyst surface (Taran et al., 2010). We are fully aware that it is difficult to compare our system with  
619 Fischer-Tropsch synthesis of methane occurring at high temperature and pressure. Yet given the indirect evidence for NO  
620 accumulation in our experiments, it may well be that preferential chemisorption/complexation of “heavy” intermediate NO  
621 occurs, which may lead to transient <sup>15</sup>N-depletion in the reactant NO<sub>2</sub><sup>-</sup> pool. Considering that the N<sub>2</sub>O concentrations measured  
622 in our experiments were comparatively low and that δ<sup>15</sup>N<sup>bulk</sup> N<sub>2</sub>O values did not noticeably change throughout the experiments,  
623 it is unlikely that N<sub>2</sub>O is the final product, and formation of N<sub>2</sub> via abiotic interactions between NO<sub>2</sub><sup>-</sup> and NO may is probably  
624 also be involved (Doane, 2017; Phillips et al., 2016). Considering the accumulated product equation (see e.g. Casciotti et al.,  
625 2011) and estimate of the δ<sup>15</sup>N<sup>bulk</sup> value of N<sub>2</sub>O, although N<sub>2</sub>O is clearly not the only product here, can at least be calculated  
626 for the mineral plus DB amended setups. The calculated Indeed, if accumulated as final product, the δ<sup>15</sup>N<sup>bulk</sup>-N<sub>2</sub>O value at  
627 the end of the incubation should be therefore yield ~-332.9‰ (according closed-system accumulated-product Rayleigh

**Kommentiert [AV6]:** Used:  
 $D^{15}N_{pA} = d^{15}N_{s,0} - 15e^*f \ln(f)/(1-f)$   
See  
[https://www.who.edu/cms/files/jhayes/2005/9/IsoCalcs30Sept04\\_5183.pdf](https://www.who.edu/cms/files/jhayes/2005/9/IsoCalcs30Sept04_5183.pdf)  
Equation 46  
Or Casciotti 2011 Equation 11.3



628 dynamics), which is roughly is significantly 10% higher than what has been what we have measured (~ -50 ±6 ‰).  
 629 Unfortunately, due to the branching effect occurring during reduction (i.e. O atoms get plucked off and lost along the reaction);  
 630 this estimation cannot be performed for the  $\delta^{18}\text{O}-\text{N}_2\text{O}$  values. Hence, considering all these attempts to understand this complex  
 631 system, it becomes very clear seems that  $\text{N}_2\text{O}$  is likely to is indeed meddling with the overall reaction dynamics either as an  
 632 intermediate or as a side product, and can thereby influence the overall N and O isotope dynamics in highly complex ways.



633  
 634 Figure 8: Conceptual figure depicting the proposed reaction mechanisms and feedbacks between the different N species during  
 635 chemodenitrification induced by the presence of a mineral surface (lower left corner) or (dead) biomass (upper right corner).  
 636 Adsorption of  $\text{Fe}^{2+}$  (directly or via complexation by  $\text{OH}^-$ ) as well as  $\text{NO}_2^-$  could catalyse a direct reaction between both. In addition,  
 637  $\text{NO}_2^-$  adsorption onto the  $\text{Fe(II)}$  mineral might also induce disproportionation, leading to  $\text{NO}_x$  formation. These formed  
 638 intermediates, although transitory, may impact the overall reaction dynamics by e.g. complex formation (i.e.  $[\text{NO}-\text{Fe}^{2+}]$ ) or direct  
 639  $\text{Fe(II)}$  oxidation. The produced  $\text{Fe(III)}$  might induce another feedback loop (autocatalysis) resulting in further  $\text{Fe(II)}$  oxidation.  
 640 Similar processes are possibly induced by the presence of (dead) biomass. Adsorption and complexation of either  $\text{NO}_2^-$  and  $\text{Fe}^{2+}$   
 641 would enhance the reaction between both. In addition, the presence of organic acids would decrease the pH locally and thereby  
 642 promote and accelerate  $\text{NO}_2^-$  disproportionation and thus additionally enhance  $\text{Fe(II)}$  oxidation. Our results suggest that  $\text{NO}_2^-$   
 643 reduction results in an KIE, which should influence the isotopic composition of  $\text{NO}$ .  $\text{N}_2\text{O}$  here is an intermediate, the isotopic  
 644 composition of which is mainly influenced by an EIE between  $\text{NO}$  and  $\text{N}_2\text{O}$ . The low  $\text{N}_2\text{O}$  yields as well as the  $\text{N}_2\text{O}$  isotopic results  
 645 (bulk, SP) clearly suggests that  $\text{N}_2$  is produced abiotically.

- Formatiert: Durchgestrichen
- Kommentiert [ML7]: This does not relly help and improve things...it is not clear what you want to say here.
- Kommentiert [ML8]: We do not need this to make the point
- Formatiert: Durchgestrichen
- Kommentiert [AV9]: Corrected (colours were missing for some of the bonds)

646

## 647 5. Conclusions and outlook

648 In the absence of any clear (genetic) evidence for enzymatic NDFeO from cultures (e.g. *Acidovorax* sp. strain BoFeN1),  
649 heterotrophic denitrification/NO<sub>3</sub><sup>-</sup> reduction coupled to abiotic oxidation of Fe(II) with the NO<sub>2</sub><sup>-</sup> has been presented as the most  
650 reasonable explanation for NDFeO. Here we investigated the second, abiotic step, clearly demonstrating that Fe-associated  
651 abiotic NO<sub>2</sub><sup>-</sup> reduction can be catalysed by mineral and organic phases under environmentally relevant conditions, as found  
652 for example in soils and aquifers. Our results confirm that reactive surfaces play a major role with regards to the reaction  
653 between NO<sub>2</sub><sup>-</sup> and Fe(II) and that surface-catalysed chemodenitrification appears to not only contribute to the production of  
654 the greenhouse gas N<sub>2</sub>O in environments hosting active cycling of Fe and N, but also to an abiotic production of N<sub>2</sub>. In order  
655 to understand the mechanistic details of Fe-coupled chemodenitrification, natural-abundance measurements of reactive-N  
656 isotope ratios may help distinguish between abiotic and biotic reactions during NDFeO. Our results, however, indicate that the  
657 potential of coupled N and O isotope measurements to determine the relative importance of Fe-induced N-transformations in  
658 natural environments is somewhat limited. Considering, for example, the apparent inverse N isotope effect in the mineral-only  
659 experiments, our studies show that the NO<sub>2</sub><sup>-</sup> N vs. O isotope systematics seem to contrast distinctly between biotic and abiotic  
660 NO<sub>2</sub><sup>-</sup> reduction, potentially permitting the disentanglement of the biotic versus abiotic processes. N<sub>2</sub>O SP values seem to be  
661 less diagnostic with regards to discriminating between chemodenitrification-derived N<sub>2</sub>O and N<sub>2</sub>O that is produced during  
662 microbial NO<sub>2</sub><sup>-</sup> reduction. Our results suggest that both the reaction between Fe(II) and reactive N species, as well as the  
663 resulting isotope effects, are dependent on the reactive surfaces available. The presence of organic material seems to enhance  
664 NO<sub>2</sub><sup>-</sup> reduction and, to a lesser extent also N<sub>2</sub>O production, leading to the enrichment in <sup>15</sup>N in the residual NO<sub>2</sub><sup>-</sup>, as predicted  
665 by Rayleigh-type kinetic N isotope fractionation. In the presence of only Fe(II) minerals, NO<sub>2</sub><sup>-</sup> reduction rates are significantly  
666 lower, and net N and O isotope effects are not governed by kinetic isotope fractionation only, but also by isotope equilibrium  
667 fractionation during exchange with the ambient mineral phase and/or the ambient water (in the case of O isotopes). While N<sub>2</sub>O  
668 production was significant, the N<sub>2</sub>O yields were below 5%, suggesting that a significant fraction of the NO<sub>2</sub><sup>-</sup> reduced is at least  
669 transiently transformed to NO and possibly N<sub>2</sub>. This transient pool of NO possibly stands in quasi-equilibrium with other  
670 intermediates (i.e. HNO, NO<sub>2</sub>(g)) or complexes (i.e. Fe-NO), and may thereby impact the overall reaction kinetics as well.  
671 We speculate that the transient accumulation of NO represents an important constraint both on overall reaction kinetics as well  
672 as on the N<sub>2</sub>O isotopic signature (or Δ<sup>15</sup>N), an aspect that should be verified in future work. Such work may include the  
673 quantification of N<sub>2</sub> (and its N isotopic composition), which will help to assess to what extent (i) Fe-mineral surface-induced  
674 chemodenitrification leads to the formation of a transient pool of NO and is driven by the catalytically induced abiotic reaction  
675 between Fe(II) and NO<sub>2</sub><sup>-</sup>, or if (ii) NO is actually the main oxidizing agent of Fe(II).  
676 Our data revealed further complexity with regards to N and O isotope effects during Fe-coupled chemodenitrification than  
677 previously reported. We argue that its isotopic imprint depends on the substrate concentration, the presence of reactive surfaces

678 or other catalysts, the mechanisms induced by these catalysts (e.g. surface complexation), and putatively on the intermediates  
679 as well as on the product present at the end of the experiments. The multifaceted control on coupled N and O isotope  
680 systematics in reactive N species may explain the discrepancies observed between our and previous work (e.g., with regards  
681 to  $^{15}\text{E}:$  $^{18}\text{E}$  ratios; Grabb et al. 2017). Clearly, one has to be realistic with regards to using  $\text{NO}_2^-$  and/or  $\text{N}_2\text{O}$  and O isotope  
682 measurements to provide constraints on the relative importance of chemodenitrification under natural conditions. Yet, at this  
683 point, there is only a very limited number of studies on the isotope effects of chemodenitrification, and with the results  
684 presented here, we expand the body of work that aims at using stable isotope measurements to assess the occurrence of  
685 chemodenitrification in denitrifying environments. More work on the controls of stable isotope systematics of  
686 chemodenitrification, in particular on the role of reactive, and potentially cryptic, intermediate N species, and of O isotope  
687 exchange, will improve our ability to more quantitatively trace Fe-coupled nitrite reduction and  $\text{N}_2\text{O}$  production in natural Fe-  
688 rich soil or sedimentary environments.

#### 689 **Data availability**

690 Data can be accessed upon request to the corresponding author.

#### 691 **Author contributions**

692 AAK initiated the project. MFL and AAK supervised the project. ANV designed and conducted all experiments. Isotope  
693 measurements as well as data analysis were performed by ANV under the supervision of MFL. JMB conducted Mössbauer  
694 measurements and data analysis. PAN supervised and performed all  $\text{N}_2\text{O}$  concentration determination measurements. ANV,  
695 SDW and MFL interpreted the data and prepared the paper with inputs from all other co-authors.

#### 696 **Competing interests**

697 The authors declare that they have no conflict of interest.

#### 698 **Acknowledgements**

699 Special thanks go to Karen L. Casciotti (Stanford University) for helping with the correction of the  $\text{N}_2\text{O}$  isotope data. Thanks  
700 to Cindy-Louise Lockwood and Toby Samuels for corrections and comments on earlier-versions of the manuscript, and to  
701 Viola Warter, Elizabeth Tomaszewski for fruitful discussions on abiotic chemistry and mineral reactions. Markus Maisch is  
702 thanked for his help with the preparation of the Mössbauer samples and Louis Rees for his help with cultivating *S. oneidensis*  
703 MR-1.

Formatiert: Schriftart: Kursiv

704 **Funding**

705 This research was supported by the Deutsche Forschungsgemeinschaft - DFG (Grants GRK 1708 Molecular principles of  
706 bacterial survival strategies), and through funds from the University of Basel, Switzerland.

707 **References**

- 708 Anderson, I. C. and Levine, J. S.: Relative Rates of Nitric Oxide and Nitrous Oxide Production by Nitrifiers, Denitrifiers, and  
709 Nitrate Respirers, *Appl. Environ. Microbiol.*, 51(5), 938–945 [online] Available from:  
710 <http://www.ncbi.nlm.nih.gov/pmc/articles/PMC238991/>, 1986.
- 711 Andrews, S. C., Robinson, A. K., Rodriguez-Quinones, F. and Rodríguez-Quinones, F.: Bacterial iron homeostasis, *Fems*  
712 *Microbiol. Rev.*, 27(2–3), 215–237, doi:10.1016/s0168-6445(03)00055-x, 2003.
- 713 Baumgärtner, M. and Conrad, R.: Role of nitrate and nitrite for production and consumption of nitric oxide during  
714 denitrification in soil, *Fems Microbiol. Lett.*, 101(1), 59–65, doi:10.1111/j.1574-6968.1992.tb05762.x, 1992.
- 715 Braun, V. and Hantke, K.: *The Tricky Ways Bacteria Cope with Iron Limitation*, pp. 31–66, Springer, Dordrecht., 2013.
- 716 Buchwald, C. and Casciotti, K. L.: Isotopic ratios of nitrite as tracers of the sources and age of oceanic nitrite, *Nat. Geosci.*,  
717 6(4), 308–313, doi:10.1038/ngeo1745, 2013.
- 718 Buchwald, C., Grabb, K., Hansel, C. M. and Wankel, S. D.: Constraining the role of iron in environmental nitrogen  
719 transformations: Dual stable isotope systematics of abiotic NO<sub>2</sub>- reduction by Fe(II) and its production of N<sub>2</sub>O, *Geochim.*  
720 *Cosmochim. Acta*, 186, 1–12, doi:<http://dx.doi.org/10.1016/j.gca.2016.04.041>, 2016.
- 721 Casciotti, K. L.: Inverse kinetic isotope fractionation during bacterial nitrite oxidation, *Geochim. Cosmochim. Acta*, 73(7),  
722 2061–2076, doi:10.1016/j.gca.2008.12.022, 2009.
- 723 Casciotti, K. L. and McIlvin, M. R.: Isotopic analyses of nitrate and nitrite from reference mixtures and application to Eastern  
724 Tropical North Pacific waters, *Mar. Chem.*, 107(2), 184–201, doi:10.1016/j.marchem.2007.06.021, 2007.
- 725 Casciotti, K. L., Boehlke, J. K., McIlvin, M. R., Mroczkowski, S. J., Hannon, J. E., Böhlke, J. K., McIlvin, M. R.,  
726 Mroczkowski, S. J. and Hannon, J. E.: Oxygen isotopes in nitrite: Analysis, calibration, and equilibration, *Anal. Chem.*, 79(6),  
727 2427–2436, doi:10.1021/ac061598h, 2007.
- 728 Casciotti, K. L., Buchwald, C., Santoro, A. E. and Frame, C.: Assessment of nitrogen and oxygen isotopic fractionation during  
729 nitrification and its expression in the marine environment, in *Methods in Enzymology*, vol. 486, edited by M. G. Klotz, pp.  
730 253–280, Academic Press Inc., 2011.
- 731 Chakraborty, A., Roden, E. E., Schieber, J. and Picardal, F.: Enhanced growth of *Acidovorax* sp. strain 2AN during nitrate-  
732 dependent Fe(II) oxidation in batch and continuous-flow systems., *Appl. Environ. Microbiol.*, 77(24), 8548–56,  
733 doi:10.1128/AEM.06214-11, 2011.
- 734 Charlet, L., Wersin, P. and Stumm, W.: Surface charge of MnCO<sub>3</sub> and FeCO<sub>3</sub>, *Geochim. Cosmochim. Acta*, 54(8), 2329–  
735 2336, doi:10.1016/0016-7037(90)90059-T, 1990.

736 Chen, D., Liu, T., Li, X., Li, F., Luo, X., Wu, Y. and Wang, Y.: Biological and chemical processes of microbially mediated  
737 nitrate-reducing Fe(II) oxidation by *Pseudogulbenkiania* sp. strain 2002, *Chem. Geol.*, 476, 59–69,  
738 doi:10.1016/j.chemgeo.2017.11.004, 2018.

739 Choi, P. S., Naal, Z., Moore, C., Casado-Rivera, E., Abruna, H. D., Helmann, J. D. and Shapleigh, J. P.: Assessing the Impact  
740 of Denitrifier-Produced NO on other bacteria, *Appl. Environ. Microbiol.*, 72(3), 2200–2205, doi:10.1128/aem.72.3.2200-  
741 2205.2006, 2006.

742 Van Cleemput, O. and Samater, A.: Nitrite in soils: accumulation and role in the formation of gaseous N compounds, *Fertil.*  
743 *Res.*, 45(1), 81–89, doi:10.1007/BF00749884, 1995.

744 Coby, A. J. and Picardal, F. W.: Inhibition of NO<sub>3</sub>- and NO<sub>2</sub>- reduction by microbial Fe(III) reduction: Evidence of a reaction  
745 between NO<sub>2</sub>- and cell surface-bound Fe<sup>2+</sup>, *Appl. Environ. Microbiol.*, 71(9), 5267–5274, doi:10.1128/aem.71.9.5267-  
746 5274.2005, 2005.

747 Cornell, R. M. and Schwertmann, U.: *The Iron Oxides: Structure, Properties, Reactions, Occurrences and Uses*, 2nd ed., Wiley-  
748 VCH., 2003.

749 Dai, Y.-F., Xiao, Y., Zhang, E.-H., Liu, L.-D., Qiu, L., You, L.-X., Dummi Mahadevan, G., Chen, B.-L. and Zhao, F.: Effective  
750 methods for extracting extracellular polymeric substances from *Shewanella oneidensis* MR-1, *Water Sci. Technol.*, 74(12),  
751 2987–2996, doi:10.2166/wst.2016.473, 2016.

752 Delahay, P., Pourbaix, M. and Rysselberghe, P. Van: POTENTIAL-pH DIAGRAMS', *J. Chem. Educ.* [online] Available  
753 from: <https://pubs.acs.org/doi/pdfplus/10.1021/ed027p683> (Accessed 20 April 2018), 1950.

754 Dhakal, P.: Abiotic nitrate and nitrite reactivity with iron oxide minerals, University of Kentucky., 2013.

755 Dhakal, P., Matocha, C. J., Huggins, F. E. and Vandivere, M. M.: Nitrite Reactivity with Magnetite, *Environ. Sci. Technol.*,  
756 47(12), 6206–6213, doi:10.1021/es304011w, 2013.

757 Doane, T. A.: The Abiotic Nitrogen Cycle, *ACS Earth Sp. Chem.*, 1(7), 411–421, doi:10.1021/acsearthspacechem.7b00059,  
758 2017.

759 Elsner, M.: Stable isotope fractionation to investigate natural transformation mechanisms of organic contaminants: principles,  
760 prospects and limitations, *J. Environ. Monit.*, 12(11), 2005–2031, doi:10.1039/c0em00277a, 2010.

761 Elsner, M., Schwarzenbach, R. P. and Haderlein, S. B.: Reactivity of Fe(II)-Bearing Minerals toward Reductive  
762 Transformation of Organic Contaminants, *Environ. Sci. Technol.*, 38(3), 799–807, doi:10.1021/es0345569, 2004.

763 Expert, D.: Iron, an Element Essential to Life, in *Molecular Aspects of Iron Metabolism in Pathogenic and Symbiotic Plant-  
764 Microbe Associations*, pp. 1–6, Springer, Dordrecht., 2012.

765 Fowle, D. A. and Konhauser, K. O.: *Microbial Surface Reactivity*, pp. 614–616, Springer, Dordrecht., 2011.

766 Frame, C. H. and Casciotti, K. L.: Biogeochemical controls and isotopic signatures of nitrous oxide production by a marine  
767 ammonia-oxidizing bacterium, *Biogeosciences*, 7(9), 2695–2709, doi:10.5194/bg-7-2695-2010, 2010.

768 Fry, B.: *Stable Isotope Ecology*, 3rd ed., Springer Science+Business Media, LLC, New York., 2006.

769 Goretski, J. and Hollocher, T. C.: Trapping of nitric oxide produced during denitrification by extracellular hemoglobin, *J. Biol.*

770 Chem., 263(5), 2316–2323 [online] Available from: <http://www.jbc.org/content/263/5/2316.abstract>, 1988.

771 Gorski, C. A. and Scherer, M. M.: Fe<sup>2+</sup> sorption at the Fe oxide-water interface: A revised conceptual framework, in *Aquatic*  
772 *Redox Chemistry*, vol. 1071, edited by P. G. Tratnyek, T. J. Grundl, and S. B. Haderlein, pp. 315–343, ACS Publications.,  
773 2011.

774 Grabb, K. C., Buchwald, C., Hansel, C. M. and Wankel, S. D.: A dual nitrite isotopic investigation of chemodenitrification by  
775 mineral-associated Fe(II) and its production of nitrous oxide, *Geochim. Cosmochim. Acta*, 196, 388–402 [online] Available  
776 from: <https://www.sciencedirect.com/science/article/pii/S0016703716306044> (Accessed 28 March 2019), 2017.

777 Granger, J. and Sigman, D. M.: Removal of nitrite with sulfamic acid for nitrate N and O isotope analysis with the denitrifier  
778 method, *Rapid Commun. Mass Spectrom.*, 23(23), 3753–3762, doi:10.1002/rcm.4307, 2009.

779 Granger, J., Sigman, D. M., Lehmann, M. F. and Tortell, P. D.: Nitrogen and oxygen isotope fractionation during dissimilatory  
780 nitrate reduction by denitrifying bacteria, *Limnol. Oceanogr.*, 53(6), 2533–2545, doi:10.4319/lo.2008.53.6.2533, 2008.

781 Granger, J., Karsh, K. L., Guo, W., Sigman, D. M. and Kritee, K.: The nitrogen and oxygen isotope composition of nitrate in  
782 the environment: The systematics of biological nitrate reduction, *Geochim. Cosmochim. Acta*, 73(13), A460–A460, 2009.

783 Halder, S., Yadav, K. K., Sarkar, R., Mukherjee, S., Saha, P., Haldar, S., Karmakar, S. and Sen, T.: Alteration of Zeta potential  
784 and membrane permeability in bacteria: a study with cationic agents., *Springerplus*, 4, 672, doi:10.1186/s40064-015-1476-7,  
785 2015.

786 He, H., Zhang, S., Zhu, C. and Liu, Y.: Equilibrium and kinetic Si isotope fractionation factors and their implications for Si  
787 isotope distributions in the Earth's surface environments, *Acta Geochim.*, 35(1), 15–24, doi:10.1007/s11631-015-0079-x,  
788 2016a.

789 He, S., Tominski, C., Kappler, A. A., Behrens, S. and Roden, E. E.: Metagenomic analyses of the autotrophic Fe(II)-oxidizing,  
790 nitrate-reducing enrichment culture KS, *Appl. Environ. Microbiol.*, 82(9), 2656–2668, doi:10.1128/AEM.03493-15, 2016b.

791 Heidelberg, J. F., Paulsen, I. T., Nelson, K. E., Gaidos, E. J., Nelson, W. C., Read, T. D., Eisen, J. A., Seshadri, R., Ward, N.,  
792 Methe, B., Clayton, R. A., Meyer, T., Tsapin, A., Scott, J., Beanan, M., Brinkac, L., Daugherty, S., DeBoy, R. T., Dodson, R.  
793 J., Durkin, A. S., Haft, D. H., Kolonay, J. F., Madupu, R., Peterson, J. D., Umayam, L. A., White, O., Wolf, A. M., Vamathevan,  
794 J., Weidman, J., Impraim, M., Lee, K., Berry, K., Lee, C., Mueller, J., Khouri, H., Gill, J., Utterback, T. R., McDonald, L. A.,  
795 Feldblyum, T. V., Smith, H. O., Venter, J. C., Nealson, K. H. and Fraser, C. M.: Genome sequence of the dissimilatory metal  
796 ion-reducing bacterium *Shewanella oneidensis*, *Nat. Biotechnol.*, 20(11), 1118–1123, doi:10.1038/nbt749, 2002.

797 Heil, J., Vereecken, H. and Brüggemann, N.: A review of chemical reactions of nitrification intermediates and their role in  
798 nitrogen cycling and nitrogen trace gas formation in soil, *Eur. J. Soil Sci.*, 67(1), 23–39, doi:10.1111/ejss.12306, 2016.

799 Hunkeler, D. and Elsner, M.: Principles and Mechanisms of Isotope Fractionation, in *Environmental Isotopes in*  
800 *Biodegradation and Bioremediation*, edited by M. Aelion Höhener, P., Hunkeler, D., pp. 43–76, CRC Press., 2009.

801 Ilbert, M. and Bonnefoy, V.: Insight into the evolution of the iron oxidation pathways, *Biochim. Biophys. Acta - Bioenerg.*,  
802 1827(2), 161–175, doi:<http://dx.doi.org/10.1016/j.bbabo.2012.10.001>, 2013.

803 Jamieson, J., Prommer, H., Kaksonen, A. H., Sun, J., Siade, A. J., Yusov, A. and Bostick, B.: Identifying and Quantifying the

804 Intermediate Processes during Nitrate-Dependent Iron(II) Oxidation, Environ. Sci. Technol., acs.est.8b01122,  
805 doi:10.1021/acs.est.8b01122, 2018.

806 Jones, L. C., Peters, B., Lezama Pacheco, J. S., Casciotti, K. L. and Fendorf, S.: Stable Isotopes and Iron Oxide Mineral  
807 Products as Markers of Chemodenitrification, Environ. Sci. Technol., 49(6), 3444–3452, doi:10.1021/es504862x, 2015.

808 Kampschreur, M. J. M. J., Kleerebezem, R., de Vet, W. W. J. M. J. M. and van Loosdrecht, M. C. M. M.: Reduced iron induced  
809 nitric oxide and nitrous oxide emission, Water Res., 45(18), 5945–5952, doi:http://dx.doi.org/10.1016/j.watres.2011.08.056,  
810 2011.

811 Kendall, C. and Aravena, R.: Nitrate Isotopes in Groundwater Systems, , 261–297, doi:10.1007/978-1-4615-4557-6\_9, 2000.

812 Klueglein, N. and Kappler, A. A.: Abiotic oxidation of Fe(II) by reactive nitrogen species in cultures of the nitrate-reducing  
813 Fe(II) oxidizer Acidovorax sp BoFeN1 - questioning the existence of enzymatic Fe(II) oxidation, Geobiology, 11(2), 396,  
814 doi:10.1111/gbi.12040, 2013.

815 Klueglein, N., Zeitvogel, F., Stierhof, Y.-D., Floetenmeyer, M., Konhauser, K. O., Kappler, A. A. and Obst, M.: Potential Role  
816 of Nitrite for Abiotic Fe(II) Oxidation and Cell Encrustation during Nitrate Reduction by Denitrifying Bacteria, Appl. Environ.  
817 Microbiol., 80(3), 1051–1061, doi:10.1128/aem.03277-13, 2014.

818 Lagarec, K. and Rancourt, D. G.: Extended Voigt-based analytic lineshape method for determining N-dimensional correlated  
819 hyperfine parameter distributions in Mössbauer spectroscopy, Nucl. Instruments Methods Phys. Res. Sect. B Beam Interact.  
820 with Mater. Atoms, 129(2), 266–280, doi:10.1016/S0168-583X(97)00284-X, 1997.

821 Laufer, K., Roy, H., Jørgensen, B. B. and Kappler, A. A.: Evidence for the existence of autotrophic nitrate-reducing Fe(II)-  
822 oxidizing bacteria in marine coastal sediment, Appl. Environ. Microbiol., 82(20), 6120–6131, doi:10.1128/AEM.01570-16,  
823 2016.

824 Li, W., Beard, B. L. and Johnson, C. M.: Exchange and fractionation of Mg isotopes between epsomite and saturated MgSO  
825 4 solution, Geochim. Cosmochim. Acta, 75, 1814–1828, doi:10.1016/j.gca.2011.01.023, 2011.

826 Lies, D. P., Hernandez, M. E., Kappler, A. A., Mielke, R. E., Gralnick, J. A. and Newman, D. K.: Shewanella oneidensis MR-  
827 1 uses overlapping pathways for iron reduction at a distance and by direct contact under conditions relevant for biofilms, Appl.  
828 Environ. Microbiol., 71(8), 4414–4426, doi:10.1128/aem.71.8.4414-4426.2005, 2005.

829 Liu, J. and Konermann, L.: Irreversible Thermal Denaturation of Cytochrome c Studied by Electrospray Mass Spectrometry,  
830 J. Am. Soc. Mass Spectrom., 20(5), 819–828, doi:10.1016/J.JASMS.2008.12.016, 2009.

831 Liu, J., Wang, Z., Belchik, S. M., Edwards, M. J., Liu, C., Kennedy, D. W., Merkley, E. D., Lipton, M. S., Butt, J. N.,  
832 Richardson, D. J., Zachara, J. M., Fredrickson, J. K., Rosso, K. M. and Shi, L.: Identification and Characterization of MtoA:  
833 A Decaheme c-Type Cytochrome of the Neutrophilic Fe(II)-Oxidizing Bacterium Sideroxydans lithotrophicus ES-1., Front.  
834 Microbiol., 3, 37, doi:10.3389/fmicb.2012.00037, 2012.

835 Liu, T., Chen, D., Luo, X., Li, X. and Li, F.: Microbially mediated nitrate-reducing Fe(II) oxidation: Quantification of  
836 chemodenitrification and biological reactions, Geochim. Cosmochim. Acta, doi:10.1016/J.GCA.2018.06.040, 2018.

837 Lovley, D. R.: Microbial Fe(III) reduction in subsurface environments, FEMS Microbiol. Rev., 20(3–4), 305–313,

838 doi:10.1111/j.1574-6976.1997.tb00316.x, 1997.

839 Lovley, D. R.: Electromicrobiology, *Annu. Rev. Microbiol.*, 66(1), 391–409, doi:10.1146/annurev-micro-092611-150104,

840 2012.

841 Luan, F., Liu, Y., Griffin, A. M., Gorski, C. A. and Burgos, W. D.: Iron(III)-Bearing Clay Minerals Enhance Bioreduction of

842 Nitrobenzene by *Shewanella putrefaciens* CN32, *Env. Sci Technol*, 49, 1418–1476, doi:10.1021/es504149y, 2015.

843 Luna-Zaragoza, D., Romero-Guzmán, E. T. and Reyes-Gutiérrez, L. R.: Surface and Physicochemical Characterization of

844 Phosphates Vivianite,

845  $Fe_2(PO_4)_3$  and Hydroxyapatite,  $Ca_5(PO_4)_3OH$ , *J. Miner. Mater. Charact. Eng.*,

846 08(08), 591–609, doi:10.4236/jmmce.2009.88052, 2009.

848 Mariotti, A., Germon, J. C., Hubert, P., Kaiser, P., Letolle, R., Tardieux, A. and Tardieux, P.: Experimental-Determination of

849 Nitrogen Kinetic Isotope Fractionation - Some Principles - Illustration for the Denitrification and Nitrification Processes, *Plant*

850 *Soil*, 62(3), 413–430, doi:10.1007/Bf02374138, 1981.

851 Martin, T. S. and Casciotti, K. L.: Paired N and O isotopic analysis of nitrate and nitrite in the Arabian Sea oxygen deficient

852 zone, *Deep. Res. Part I Oceanogr. Res. Pap.*, 121, 121–131, doi:10.1016/j.dsr.2017.01.002, 2017.

853 McIlvin, M. R. and Altabet, M. A.: Chemical conversion of nitrate and nitrite to nitrous oxide for nitrogen and oxygen isotopic

854 analysis in freshwater and seawater, *Anal. Chem.*, 77(17), 5589–5595, doi:10.1021/ac050528s, 2005.

855 McIlvin, M. R. and Casciotti, K. L.: Fully automated system for stable isotopic analyses of dissolved nitrous oxide at natural

856 abundance levels, *Limnol. Oceanogr. Methods*, 8(2), 54–66, doi:10.4319/lom.2010.8.54, 2010.

857 McKnight, G. M., Smith, L. M., Drummond, R. S., Duncan, C. W., Golden, M. and Benjamin, N.: Chemical synthesis of nitric

858 oxide in the stomach from dietary nitrate in humans., *Gut*, 40(2), 211–4 [online] Available from:

859 <http://www.ncbi.nlm.nih.gov/pubmed/9071933> (Accessed 18 March 2018), 1997.

860 Minguzzi, A., Fan, F.-R. F., Vertova, A., Rondinini, S. and Bard, A. J.: Dynamic potential–pH diagrams application to

861 electrocatalysts for wateroxidation, *Chem. Sci.*, 3(1), 217–229, doi:10.1039/C1SC00516B, 2012.

862 Miot, J., Remusat, L., Duprat, E., Gonzalez, A., Pont, S. and Poinso, M. M.: Fe biomineralization mirrors individual metabolic

863 activity in a nitrate-dependent Fe(II)-oxidizer, *Front. Microbiol.*, 6(SEP), 879, doi:10.3389/fmicb.2015.00879, 2015.

864 Mohn, J., Wolf, B., Toyoda, S., Lin, C.-T., Liang, M.-C., Brüggemann, N., Wissel, H., Steiker, A. E., Dyckmans, J., Szwee,

865 L., Ostrom, N. E., Casciotti, K. L., Forbes, M., Giesemann, A., Well, R., Doucett, R. R., Yarnes, C. T., Ridley, A. R., Kaiser,

866 J. and Yoshida, N.: Interlaboratory assessment of nitrous oxide isotopomer analysis by isotope ratio mass spectrometry and

867 laser spectroscopy: current status and perspectives, *Rapid Commun. Mass Spectrom.*, 28(18), 1995–2007,

868 doi:10.1002/rcm.6982, 2014.

869 Muehe, E. M., Gerhardt, S., Schink, B. and Kappler, A.: Ecophysiology and the energetic benefit of mixotrophic Fe(II)

870 oxidation by various strains of nitrate-reducing bacteria, *FEMS Microbiol. Ecol.*, 70(3), 335–343, doi:10.1111/j.1574-

871 6941.2009.00755.x, 2009.



872 Muehe, E. M., Obst, M., Hitchcock, A., Tyliczszak, T., Behrens, S., Schröder, C., Byrne, J. M., Michel, F. M., Krämer, U. and  
873 Kappler, A. A.: Fate of Cd during microbial Fe(III) mineral reduction by a novel and Cd-tolerant geobacter species, *Environ.*  
874 *Sci. Technol.*, 47(24), 14099–14109, doi:10.1021/es403365w, 2013.

875 Nelson, D. W. and Bremner, J. M.: Factors affecting chemical transformations of nitrite in soils, *Soil Biol. Biochem.*, 1(3),  
876 229–239, doi:10.1016/0038-0717(69)90023-6, 1969.

877 Niklaus, P. A., Le Roux, X., Poly, F., Buchmann, N., Scherer-Lorenzen, M., Weigelt, A. and Barnard, R. L.: Plant species  
878 diversity affects soil–atmosphere fluxes of methane and nitrous oxide, *Oecologia*, 181(3), 919–930, doi:10.1007/s00442-016-  
879 3611-8, 2016.

880 Nordhoff, M., Tominski, C., Halama, M., Byrne, J. M., Obst, M., Kleindienst, S., Behrens, S. and Kappler, A. A.: Insights into  
881 nitrate-reducing Fe(II) oxidation mechanisms through analysis of cell-mineral associations, cell encrustation, and mineralogy  
882 in the chemolithoautotrophic enrichment culture KS, *Appl. Environ. Microbiol.*, 83(13), e00752-17, doi:10.1128/AEM.00752-  
883 17, 2017.

884 Ostrom, N. E. and Ostrom, P.: *Handbook of Environmental Isotope Geochemistry*, 1st ed., edited by M. Baskaran, Springer  
885 Berlin Heidelberg, Berlin, Heidelberg., 2011.

886 Ostrom, N. E. and Ostrom, P. H.: The Isotopomers of Nitrous Oxide: Analytical Considerations and Application to Resolution  
887 of Microbial Production Pathways, in *Handbook of Environmental Isotope Geochemistry: Vol I*, edited by M. Baskaran, pp.  
888 453–476, Springer Berlin Heidelberg, Berlin, Heidelberg., 2012.

889 Ostrom, N. E., Pitt, A., Sutka, R., Ostrom, P. H., Grandy, A. S., Huizinga, K. M. and Robertson, G. P.: Isotopologue effects  
890 during N<sub>2</sub>O reduction in soils and in pure cultures of denitrifiers, *J. Geophys. Res.*, 112(G2), doi:10.1029/2006jg000287, 2007.

891 Ostrom, N. E., Gandhi, H., Coplen, T. B., Toyoda, S., Böhlke, J. K., Brand, W. A., Casciotti, K. L., Dyckmans, J., Giesemann,  
892 A., Mohn, J., Well, R., Yu, L. and Yoshida, N.: Preliminary assessment of stable nitrogen and oxygen isotopic composition of  
893 USGS51 and USGS52 nitrous oxide reference gases and perspectives on calibration needs, *Rapid Commun. Mass Spectrom.*,  
894 32(15), 1207–1214, doi:10.1002/rcm.8157, 2018.

895 Otte, J. M., Blackwell, N., Ruser, R., Kappler, A. A., Kleindienst, S. and Schmidt, C.: N<sub>2</sub>O formation by nitrite-induced  
896 (chemo)denitrification in coastal marine sediment, *Sci. Rep.*, 9(1), 10691, doi:10.1038/s41598-019-47172-x, 2019.

897 Ottley, C. J., Davison, W. and Edmunds, W. M.: Chemical catalysis of nitrate reduction by iron(II), *Geochim. Cosmochim.*  
898 *Acta*, 61(9), 1819–1828, doi:Doi 10.1016/S0016-7037(97)00058-6, 1997.

899 Pereira, C., Ferreira, N. R., Rocha, B. S., Barbosa, R. M. and Laranjinha, J.: The redox interplay between nitrite and nitric  
900 oxide: From the gut to the brain, *Redox Biol.*, 1(1), 276–284, doi:http://dx.doi.org/10.1016/j.redox.2013.04.004, 2013.

901 Phillips, R. L., Song, B., McMillan, A. M. S., Grelet, G., Weir, B. S., Palmada, T. and Tobias, C.: Chemical formation of  
902 hybrid di-nitrogen calls fungal codenitrification into question, *Sci. Rep.*, 6(1), 39077, doi:10.1038/srep39077, 2016.

903 Piasecki, W., Szymanek, K. and Charmas, R.: Fe<sup>2+</sup> adsorption on iron oxide: the importance of the redox potential of the  
904 adsorption system, *Adsorption*, doi:10.1007/s10450-019-00054-0, 2019.

905 Piepenbrock, A., Dippon, U., Porsch, K., Appel, E. and Kappler, A. A.: Dependence of microbial magnetite formation on

906 humic substance and ferrihydrite concentrations, *Geochim. Cosmochim. Acta*, 75(22), 6844–6858,  
907 doi:10.1016/j.gca.2011.09.007, 2011.

908 Price, A., Macey, M. C., Miot, J. and Olsson-Francis, K.: Draft Genome Sequences of the Nitrate-Dependent Iron-Oxidizing  
909 Proteobacteria *Acidovorax* sp. Strain BoFeN1 and *Paracoccus pantotrophus* Strain KS1, edited by J. C. Thrash, *Microbiol.*  
910 *Resour. Announc.*, 7(10), e01050-18, doi:10.1128/mra.01050-18, 2018.

911 Rakshit, S., Matocha, C. J. and Coyne, M. S.: Nitrite reduction by siderite, *Soil Sci. Soc. Am. J.*, 72(4), 1070–1077,  
912 doi:10.2136/sssaj2007.0296, 2008.

913 Rancourt, D. G. and Ping, J. Y.: Voigt-based methods for arbitrary-shape static hyperfine parameter distributions in Mössbauer  
914 spectroscopy, *Nucl. Instruments Methods Phys. Res. Sect. B Beam Interact. with Mater. Atoms*, 58(1), 85–97,  
915 doi:10.1016/0168-583X(91)95681-3, 1991.

916 Rivallan, M., Ricchiardi, G., Bordiga, S. and Zecchina, A.: Adsorption and reactivity of nitrogen oxides (NO<sub>2</sub>, NO, N<sub>2</sub>O) on  
917 Fe-zeolites, *J. Catal.*, 264(2), 104–116, doi:10.1016/j.jcat.2009.03.012, 2009.

918 Samarkin, V. A., Madigan, M. T., Bowles, M. W., Casciotti, K. L., Priscu, J. C., McKay, C. P. and Joye, S. B.: Abiotic nitrous  
919 oxide emission from the hypersaline Don Juan Pond in Antarctica, *Nat. Geosci.*, 3(5), 341–344, doi:10.1038/ngeo847, 2010.

920 Schaefer, M. V.: Spectroscopic evidence for interfacial Fe(II)- Fe(III) electron transfer in clay minerals, *Iowa Research Online*.  
921 [online] Available from: <http://ir.uiowa.edu/etd/596> (Accessed 20 March 2018), 2010.

922 Sigman, D. M., DiFiore, P. J., Hain, M. P., Deutsch, C., Wang, Y., Karl, D. M., Knapp, A. N., Lehmann, M. F. and Pantoja,  
923 S.: The dual isotopes of deep nitrate as a constraint on the cycle and budget of oceanic fixed nitrogen, *Deep. Res. Part I-*  
924 *Oceanographic Res. Pap.*, 56(9), 1419–1439, doi:10.1016/j.dsr.2009.04.007, 2009.

925 Snyder, L. R. and Adler, H. J.: Dispersion in Segmented Flow through Glass Tubing in Continuous-Flow Analysis: The Ideal  
926 Model, *Anal. Chem.*, 48(7), 1017–1022, doi:10.1021/ac60371a013, 1976.

927 Sorensen, J. and Thorling, L.: Stimulation by Lepidocrocite (Gamma-Fe<sub>2</sub>O<sub>3</sub>) of Fe(II)-Dependent Nitrite Reduction, *Geochim.*  
928 *Cosmochim. Acta*, 55(5), 1289–1294, doi:10.1016/0016-7037(91)90307-Q, 1991.

929 Stevenson, F. J., Harrison, R. M., Wetselaar, R. and Leeper, R. A.: Nitrosation of Soil Organic Matter: III. Nature of Gases  
930 Produced by Reaction of Nitrite with Lignins, Humic Substances, and Phenolic Constituents Under Neutral and Slightly Acidic  
931 Conditions I, *Soil Sci. Soc. Am. J.*, 34(3), 430, doi:10.2136/sssaj1970.03615995003400030024x, 1970.

932 Stookey, L. L.: FERROZINE - A NEW SPECTROPHOTOMETRIC REAGENT FOR IRON, *Anal. Chem.*, 42(7), 779-  
933 doi:10.1021/ac60289a016, 1970.

934 Straub, K. L., Benz, M., Schink, B. and Widdel, F.: Anaerobic, nitrate-dependent microbial oxidation of ferrous iron, *Appl.*  
935 *Environ. Microbiol.*, 62(4), 1458–1460, 1996.

936 Stumm, W. and Sulzberger, B.: The cycling of iron in natural environments: Considerations based on laboratory studies of  
937 heterogeneous redox processes, *Geochim. Cosmochim. Acta*, 56(8), 3233–3257, doi:10.1016/0016-7037(92)90301-X, 1992.

938 Sutka, R. L., Ostrom, N. E., Ostrom, P. H., Breznak, J. A., Gandhi, H., Pitt, A. J. and Li, F.: Distinguishing nitrous oxide  
939 production from nitrification and denitrification on the basis of isotopomer abundances, *Appl. Environ. Microbiol.*, 72(1),

940 638–644, doi:10.1128/Aem.72.1.638-644.2006, 2006.

941 Tanford, C.: Protein denaturation: Part c. theoretical models for the mechanism of denaturation, *Adv. Protein Chem.*, 24(C),  
942 1–95, doi:10.1016/S0065-3233(08)60241-7, 1970.

943 Taran, Y. A., Kliger, G. A., Cienfuegos, E. and Shuykin, A. N.: Carbon and hydrogen isotopic compositions of products of  
944 open-system catalytic hydrogenation of CO<sub>2</sub>: Implications for abiogenic hydrocarbons in Earth's crust, *Geochim. Cosmochim.*  
945 *Acta*, 74(21), 6112–6125, doi:10.1016/j.gca.2010.08.012, 2010.

946 Tian, T., Zhou, K., Xuan, L., Zhang, J.-X., Li, Y.-S., Liu, D.-F. and Yu, H.-Q.: Exclusive microbially driven autotrophic iron-  
947 dependent denitrification in a reactor inoculated with activated sludge, *Water Res.*, 170, 115300,  
948 doi:10.1016/j.watres.2019.115300, 2020.

949 Tiso, M. and Schechter, A. N.: Nitrate reduction to nitrite, nitric oxide and ammonia by gut bacteria under physiological  
950 conditions., *PLoS One*, 10(3), e0119712, doi:10.1371/journal.pone.0119712, 2015.

951 Tominski, C., Heyer, H., Lösekann-Behrens, T., Behrens, S. and Kappler, A. A.: Growth and Population Dynamics of the  
952 Anaerobic Fe(II)-Oxidizing and Nitrate-Reducing Enrichment Culture KS, edited by F. E. Löffler, *Appl. Environ. Microbiol.*,  
953 84(9), e02173-17, doi:10.1128/AEM.02173-17, 2018.

954 Toyoda, S. and Yoshida, N.: Determination of Nitrogen Isotopomers of Nitrous Oxide on a Modified Isotope Ratio Mass  
955 Spectrometer, , doi:10.1021/AC9904563, 1999.

956 Toyoda, S., Mutoke, H., Yamagishi, H., Yoshida, N. and Tanji, Y.: Fractionation of N<sub>2</sub>O isotopomers during production by  
957 denitrifier, *Soil Biol. Biochem.*, 37(8), 1535–1545, doi:10.1016/j.soilbio.2005.01.009, 2005.

958 Veeramani, H., Alessi, D. S., Suvorova, E. I., Lezama-Pacheco, J. S., Stubbs, J. E., Sharp, J. O., Dippon, U., Kappler, A. A.,  
959 Bargar, J. R. and Bernier-Latmani, R.: Products of abiotic U(VI) reduction by biogenic magnetite and vivianite, *Geochim.*  
960 *Cosmochim. Acta*, 75(9), 2512–2528, doi:10.1016/j.gca.2011.02.024, 2011.

961 Wankel, S. D., Ziebis, W., Buchwald, C., Charoenpong, C., De Beer, Di., Dentinger, J., Xu, Z. and Zengler, K.: Evidence for  
962 fungal and chemodenitrification based N<sub>2</sub>O flux from nitrogen impacted coastal sediments, *Nat. Commun.*, 8(1), 15595,  
963 doi:10.1038/ncomms15595, 2017.

964 Weber, K. A., Hedrick, D. B., Peacock, A. D., Thrash, J. C., White, D. C., Achenbach, L. A. and Coates, J. D.: Physiological  
965 and taxonomic description of the novel autotrophic, metal oxidizing bacterium, *Pseudogulbenkiania* sp strain 2002, *Appl.*  
966 *Microbiol. Biotechnol.*, 83(3), 555–565, doi:10.1007/s00253-009-1934-7, 2009.

967 Well, R. and Flessa, H.: Isotopologue signatures of N<sub>2</sub>O produced by denitrification in soils, *J. Geophys. Res.*, 114,  
968 doi:10.1029/2008jg000804, 2009.

969 Wenk, C. B., Frame, C. H., Koba, K., Casciotti, K. L., Veronesi, M., Niemann, H., Schubert, C. J., Yoshida, N., Toyoda, S.,  
970 Makabe, A., Zopfi, J. and Lehmann, M. F.: Differential N<sub>2</sub>O dynamics in two oxygen-deficient lake basins revealed by stable  
971 isotope and isotopomer distributions, *Limnol. Oceanogr.*, 61(5), 1735–1749, doi:10.1002/lno.10329, 2016.

972 White, G. F., Edwards, M. J., Gomez-Perez, L., Richardson, D. J., Butt, J. N. and Clarke, T. A.: Mechanisms of Bacterial  
973 Extracellular Electron Exchange, in *Advances in Microbial Physiology*, vol. 68, pp. 87–138., 2016.

974 Widdel, F. and Pfennig, N.: STUDIES ON DISSIMILATORY SULFATE-REDUCING BACTERIA THAT DECOMPOSE  
975 FATTY-ACIDS .1. ISOLATION OF NEW SULFATE-REDUCING BACTERIA ENRICHED WITH ACETATE FROM  
976 SALINE ENVIRONMENTS - DESCRIPTION OF DESULFOBACTER-POSTGATEI GEN-NOV, SP-NOV, Arch.  
977 Microbiol., 129(5), 395–400, doi:10.1007/bf00406470, 1981.

978 Widdel, F., Kohring, G.-W. and Mayer, F.: Studies on Dissimilatory Sulfate-Reducing Bacteria that Decompose Fatty Acids,  
979 Arch Microbiol, 134, 286–294 [online] Available from: <https://link.springer.com/content/pdf/10.1007/BF00407804.pdf>  
980 (Accessed 22 April 2018), 1983.

981 Wilson, W. W., Wade, M. M., Holman, S. C. and Champlin, F. R.: Status of methods for assessing bacterial cell surface charge  
982 properties based on zeta potential measurements, J. Microbiol. Methods, 43(3), 153–164, doi:10.1016/S0167-7012(00)00224-  
983 4, 2001.

984 Winther, M., Balslev-Harder, D., Christensen, S., Priemé, A., Elberling, B., Crosson, E. and Blunier, T.: Continuous  
985 measurements of nitrous oxide isotopomers during incubation experiments, Biogeosciences, 15(3), 767–780, doi:10.5194/bg-  
986 15-767-2018, 2018.

987 Wunderlin, P., Lehmann, M. F., Siegrist, H., Tuzson, B., Joss, A., Emmenegger, L. and Mohn, J.: Isotope Signatures of N<sub>2</sub>O  
988 in a Mixed Microbial Population System: Constraints on N<sub>2</sub>O Producing Pathways in Wastewater Treatment, Environ. Sci.  
989 Technol., 130118101927005, doi:10.1021/es303174x, 2013.

990 Ye, R. W., Averill, B. A. and Tiedje, J. M.: Denitrification: production and consumption of nitric oxide, Appl. Environ.  
991 Microbiol., 60(4), 1053–1058 [online] Available from: <http://www.ncbi.nlm.nih.gov/pmc/articles/PMC201439/>, 1994.

992 Zeitvogel, F., Burkhardt, C. J., Schroepel, B., Schmid, G., Ingino, P. and Obst, M.: Comparison of Preparation Methods of  
993 Bacterial Cell-Mineral Aggregates for SEM Imaging and Analysis Using the Model System of *Acidovorax* sp. BoFeN1,  
994 Geomicrobiol. J., 34(4), 317–327, doi:10.1080/01490451.2016.1189467, 2017.

995 Zhu-Barker, X., Cavazos, A. R., Ostrom, N. E., Horwath, W. R. and Glass, J. B.: The importance of abiotic reactions for  
996 nitrous oxide production, Biogeochemistry, 126(3), 251–267, doi:10.1007/s10533-015-0166-4, 2015.

997 Zumft, W. G.: Cell biology and molecular basis of denitrification, Microbiol. Mol. Biol. Rev., 61(4), 533–+ [online] Available  
998 from: <http://www.ncbi.nlm.nih.gov/pubmed/9409151> (Accessed 19 February 2018), 1997.

999 Zweier, J. L., Samouilov, A. and Kuppasamy, P.: Non-enzymatic nitric oxide synthesis in biological systems, Biochim.  
1000 Biophys. Acta - Bioenerg., 1411(2–3), 250–262, doi:10.1016/S0005-2728(99)00018-3, 1999.

1001

**Kommentiert [ML10]:** Check refs...they seem unformatted, some are messed up of only in capital letters (e.g. Widdel)